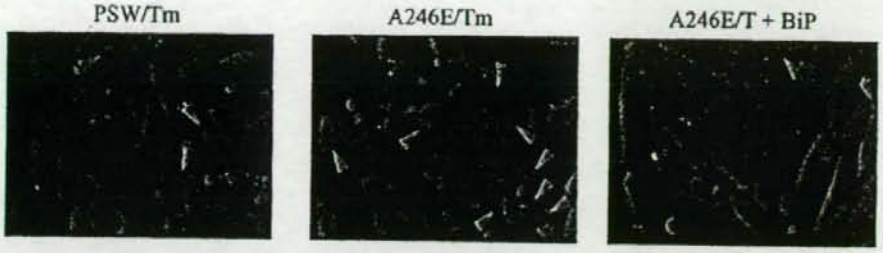


図2　プレセニリン1変異体発現細胞のERストレス脆弱性とBiP誘導によるレスキュー．プレセニリン1変異体（A246E）発現細胞は野生型（PSW）細胞に比し，ERストレス（tunicamycin: Tm）に脆弱性を示す（矢印は神経細胞死）が，あらかじめウイルスベクターを用いてBiPを発現させておくと，この脆弱性はレスキューできる．

示唆する事実である．

また，遺伝性若年性パーキンソン病の原因遺伝子であるParkinはユビキチンリガーゼであることが示され，Parkinの変異体は基質であるPeal受容体のERADを発動することができず，unfoldedなPeal受容体を溜め，ER発動のアポトーシスを招くとされる（Imai et al, 2001）．ハンチントン病などのポリグルタミン病は，CAGのリピートが異常に伸張したために神経変性を呈する疾患であるが，伸張したポリグルタミンはプロテオソームの機能低下をきたし，ERストレスを惹起し，ASK1を活性化してJNKを介するアポトーシスが発動することが示されている．以上のように，UPRの異常は神経変性疾患の共通した病理因子である可能性が示唆されている．

### 分子シャペロン誘導剤開発

以上の知見から，UPRを人為的に活性化することは，アルツハイマー病をはじめとする神経変性疾患の治療につながる可能性が考えられる．我々の過去の検討で，BiPを発現するウイルスベクターを神経細胞にあらかじめ感染させておくと，プレセニリン1変異体によるERストレス脆弱性が改善した結果を得ている（図2）．そこで我々は，UPRのうち分子シャペロン誘導に着目し，分子シャペロンBiP誘導剤の検索を行った．BiPのプロモーター配列を利用してBiPレポーターシステムを構築し，コンパウンドライブラリーをハイスループットスクリーニングにて検索し，最もBiPのメッセージを誘導するコンパウンドBiP inducer X（BIX）を得た．このBIXを神経芽細胞腫SK-N-SHに投与すると，BIXの濃度依存的にBiPを誘導することが示されたが，古典的なERストレス誘導剤であるthapsigargin等が誘導するようなBiPの高レベルよりは低く観察された．また，BIXによるBiP誘導は，投与4時間後から起こり，6時間後をピークに減衰していくことが観察された．以上の観察されたメッセージレベルのBiP誘導には，BiP蛋白発現を伴っていることが，ウェスタンブロット法にて確認された．

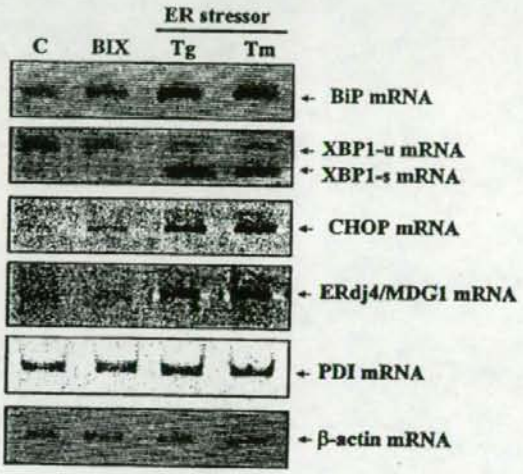


図3　BIXのBiP誘導効果とその他のERストレス．BIXはBiPのみを誘導し，thapsigargin（Tg）やtunicamycin（Tm）などのERストレッサーが誘導するようなその他のERストレス誘導分子は誘導しない．

このBIXが，もしBiP以外のERストレスによって発現される分子を活性化すれば，ERストレスによるアポトーシスにつながりかねず，治療法とはなり得ない．そこで，BiP以外のERストレス分子XBP1，CHOP，ERdj4/MDG1，PDIの活性化について，BIXの効果を検討した．BIXをSK-N-SH細胞に投与しても，BiPは誘導するが，XBP1のスプライシング（活性化），CHOPの誘導，ERdj4/MDG1の誘導，PDIの誘導は起きないことが確認された（図3）．また，BiP誘導と相対する蛋白翻訳抑制を起こすeIF2αのリン酸化についてもBIXの効果を検討したが，そのリン酸化は観察されなかった．以上の結果から，BIXはBiPのみを誘導し，他のERストレス反応分子を誘導しないことが示された．

### BIXの神経細胞におけるERストレス保護作用

BIXのERストレス保護作用を検討する目的で，BIXをSK-N-SH細胞の培地に添加し，12時間後にtunicamycin

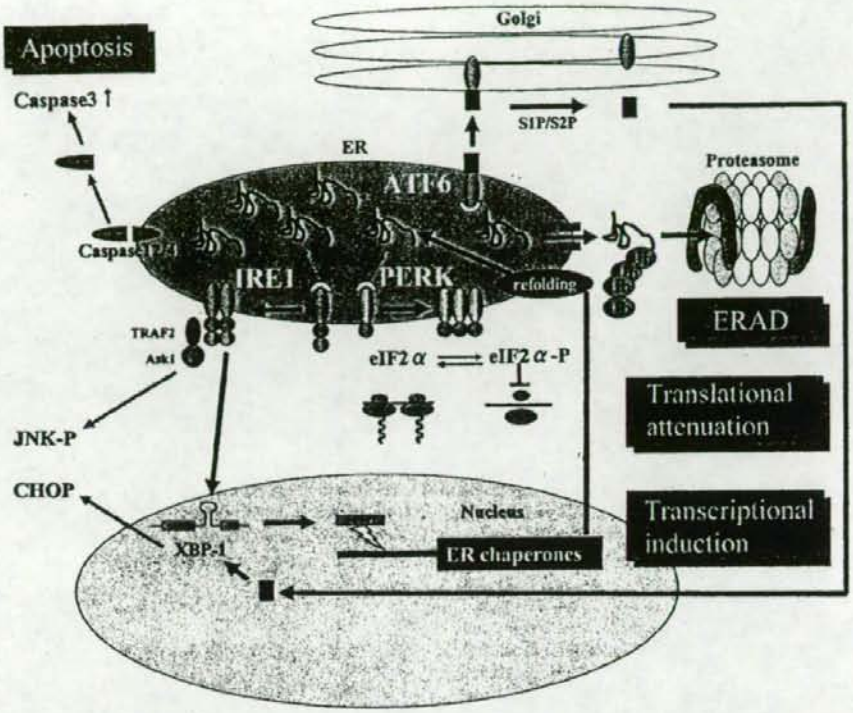


**図1** 小胞体（ER）ストレス反応（unfolded protein response: UPR）とアポトーシス．

### ERストレストランスデューサー（図1）

UPRは，ER内のunfolded proteinの蓄積を感知することから始動する．現在まで，unfolded proteinのセンサーとしてER膜上のIRE1，PERK，ATF6が報告されている．IRE1は，二量体形成と自己リン酸化を経て，XBP-1のalternative splicingを起こし，成熟型のXBP-1を生じさせる（Yoshida et al, 2001）．この成熟型XBP-1は，GRP78/BiP等の分子シャペロンのプロモーターに働き，分子シャペロンを誘導する（Wang et al, 1998）．PERKは，多量体化と自己リン酸化を経て，eIF2$\alpha$をリン酸化する（Harding et al, 1999）．このリン酸化されたeIF2$\alpha$は43S initiation complexの形成を阻害し，翻訳開始を阻害する．ATF6は，ゴルジに運ばれ，S1PおよびS2Pによって細胞質側の膜貫通領域近傍で切断を受け，できたN末端領域がXBP1の転写を促進して分子シャペロンの誘導につながる（Haze et al, 1999）．これら3つのトランスデューサーは，非ストレス下ではGRP78/BiPが結合しており，unfolded proteinのER内での蓄積に際しその結合がはずれ，UPRが開始されるという共通の機序が想定されている．

### ERストレスと神経変性疾患

我々は，家族性アルツハイマー病の主要な原因遺伝子であるプレセニリン1がERに局在することから，ERストレスとプレセニリン1変異体の関係について検討した．プレセニリン1変異体発現神経細胞は，ERストレスに脆弱であることが示され，ERストレス下における分子シャペロンBiPの誘導が抑制されることが見いだされた．プレセニリン1変異体神経細胞のUPRを検討すると，IRE1，PERK，ATF6全てのトランスデューサーの活性化が障害されており，UPR抑制のためにERストレス脆弱性をきたしていることが示唆された（Katayama et al, 1999, 2001; Yasuda et al, 2002）．また，プレセニリン1変異体神経細胞にUPRの1つであるBiPをウイルスベクターにより発現させておくと，ERストレス脆弱性をレスキューできることも示された（図2）．したがって，プレセニリン1変異による家族性アルツハイマー病の神経変性には，UPR障害が関与すると考えられる．実際，家族性アルツハイマー病患者脳ではBiPの発現が低いことが観察されており，おもしろいことに孤発性AD患者脳でもBiP発現が低下していることが観察された．これは，ADの神経変性に共通してBiP誘導障害，すなわちUPR障害が関与することを

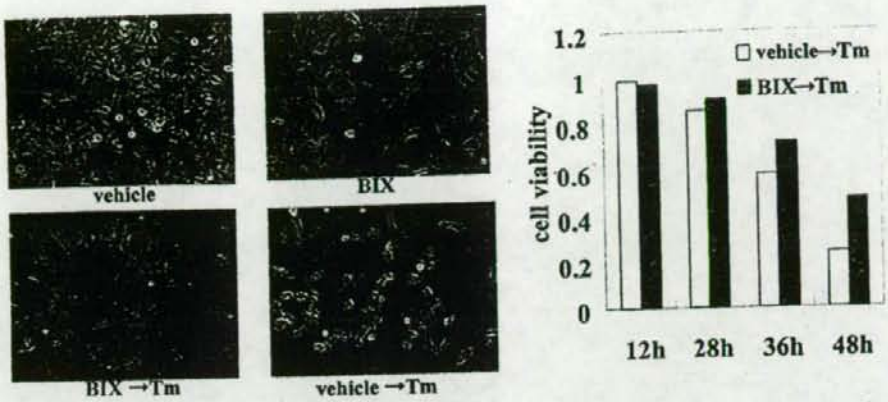


図4 BIX の抗 ER ストレス効果．BIX を 12 時間前に前投与しておくと，vehicle 投与神経細胞に比し，ER ストレス（tunicamycin: Tm）による神経細胞死を抑制できる．

を投与して ER ストレスをかけた．BIX を投与していない細胞では，tunicamycin 投与後 36 時間後より細胞死が観察されたが，BIX 投与細胞では有意な細胞死の減少が観察された（図 4）．ER ストレスから誘導されるアポトーシスで活性化されるカスペース 4 についてウェスタンブロット法で検討したところ，BIX 投与細胞ではその活性化が抑制されていることが確認され，BIX は ER ストレスによるアポトーシスを抑制し，神経細胞を保護することが示された．

### BIX の脳虚血モデルにおける効果

脳虚血は ER ストレスを惹起するので，BIX の効果を検証する *in vivo* の実験系として，マウスの中大脳動脈閉塞（MCAO）モデルを採用した．BIX のマウス脳室内投与は，6 時間後で脳実質内の BiP を誘導することが確認された．今回は，脳虚血 30 分前に BIX を脳室内投与し，MCAO 24 時間後に薬剤の効果を検討した．通常 MCAO 後 24 時間では，歩行不可，反対側への旋回運動，反対側前足の伸展障害，あるいは神経症状なしのいずれかの神経障害が認められ，多くのマウスは旋回運動程度の神経障害を示すが，BIX 投与マウスでは神経障害は軽度となり，前足の伸展障害程度を示していた．MCAO 24 時間後の脳切片を作製し，TTC 染色により脳梗塞部位の計測を行ったところ，BIX 投与マウスでは脳梗塞部位面積の有意な減少が認められ，特に梗塞周辺領域（penumbra）の減少が顕著であった．また，MCAO 24 時間後の脳浮腫についても検討したところ，BIX 投与マウスでは有意に脳浮腫が軽減されていた．これらの結果は，BIX の脳室内前投与が MCAO による脳梗塞の侵襲を軽減して神経症状発現を抑えうることを示している．

BIX の効果は，penumbra の減少に顕著に認められたが，その部位での ER ストレスによるアポトーシスについて検討した．アポトーシス発現細胞を見るために脳切片を TUNEL 染色したところ，BIX 投与マウスの penumbra における TUNEL 陽性細胞は有意に減少していることが観察された．さらに，ER ストレスによるアポトーシス誘導分子である CHOP の誘導について *in situ* hybridization にて検討したところ，CHOP の誘導も BIX 投与マウスの penumbra において有意に抑制されていることが観察された．これらのことから，BIX 投与は penumbra の ER ストレスを軽減し，それによるアポトーシスを抑制することで梗塞巣の増大を抑え，また *in vivo* においても，BIX は ER ストレスによるアポトーシスに効果があることを示している．

### 文 献

Bonifacino, J. S. and Weissman, A. M. (1998) Ubiquitin and the control of protein fete in the secretory and endocytic pathways. Annu Rev Cell Dev Biol, 14: 19-57.

Friedman, A. D. (1996) GADD153/CHOP, a DNA damage-inducible protein, reduced CAAT/Enhancer binding protein activities and increased apoptosis in 32D cl3 myeloid cells. Cancer Res, 56: 3250-3256.

Harding, H. P., Zhang, Y. and Ron, D. (1999) Protein translation and folding are coupled by an endoplasmic-reticulum-resident kinase. Nature, 397: 271-274.

Haze, K., Yoshida, H., Yanagi, H., Yura, T. and Mori, K. (1999) Mammalian transcription factor ATF6 is synthesized as a transmembrane protein and activated by proteolysis in response to endoplasmic reticulum stress. Mol Biol Cell, 10: 3787-3799.

Hitoffhi, J., Katayama, T., Eguchi, Y., Kudo, T., Taniguchi, M., Koyama, Y., Manabe, T., Yamagishi, S., Bando, Y., Imaizumi, K., Tsujimoto, Y. and Tohyama, M. (2004) Involvement of caspase-4 in endoplasmic reticulum stress-induced apoptosis and Aβ-induced cell death. J Cell Biol, 165: 347-356.

Imai, Y., Soda, M., Inoue, H., Hattori, N., Mizuno, Y. and Takahashi, R. (2001) An unfolded putative transmembrane polypeptide, which can lead to endoplasmic reticulum stress, is a substrate of parkin. Cell, 105: 891-902.

Katayama, T., Imaizumi, K., Sato, N., Miyoshi, K., Kudo, T., Hitomi,

J., Morihara, T., Yoneda, T., Gomi, F., Mori, Y., Nakano, Y., Takeda, J., Tsuda, T., Itoyama, Y., Murayama, O., Takashima, A., St George-Hyslop, P., Takeda, M. and Tohyama, M. (1999) Presenilin-1 mutations downregulate the signalling pathway of the unfolded-protein response. Nat Cell Biology, 8: 479–485.

Katayama, T., Imaizumi, K.,.Honda, A., Yoneda, T., Kudo, T., Takeda, M., Mori, K., Rozmahel, R., Fraser, P., St.George-Hyslop, P. and Tohyama, M. (2001) Disturbed activation of endoplasmic reticulum stress transducers by familial Alzheimer's disease-linked presenilin 1 mutations. J Biol Chem, 276: 43446–43454.

Nakagawa, T., Zhu, H., Morishima, N., Li, E., Xu, J., Yankner, B. A. and Yuan, J. (2000) Caspase-12 mediates endoplasmic-reticulum-specific apoptosis and cytotoxicity by amyloid-$\beta$. Nature, 403: 98–103.

Nishitoh, H., Matsuzawa, A., Tobiume, K., Saegusa, K., Takeda, K., Inoue, K., Hori, S., Kakizuka, A. and Ichijo, H. (2002) ASK1 is essential for endoplasmic reticulum stress-induced neuronal cell death triggered by expanded polyglutamine repeats. Genes Dev, 16: 1345–1355.

Sidrauski, C., Chapman, R. and Walteret, P. (1998) The unfolded protein response: An intracellular signalling pathway with many surprising features. Trends Cell Biol, 8: 245–249.

Wang X.-Z., Harding, H. P., Zhang, Y., Jolicoeur, E. M., Kuroda, M. and Ron, D. (1998) Cloning of mammalian Ire1 reveals diversity in the ER stress responses. EMBO J, 17: 5708–5717.

Yasuda, Y., Kudo, T., Katayama, T., Imaizumi, K., Yatera, M., Okochi, M., Yamamori, H., Matsumoto, N., Kida, T., Fukumori, A., Okumura, M., Tohyama, M. and Takeda, M. (2002) FAD-linked presenilin-1 mutants impede translation regulation under ER stress. Biochem Biophys Res Commun, 296: 313–318.

Yoshida, H., Matsui, T., Yamamoto, A., Okada, T. and Mori, K. (2001) XBP1 mRNA is induced by ATF6 and spliced by IRE1 in response to ER stress to produce a highly active transcription factor. Cell, 107: 881–891.

**Abstract:** Takashi KUDO[*1], Kazunori IMAIZUMI[*2] and Hideaki HARA[*3] ([*1]Department of Psychiatry, Osaka University Graduate School of Medicine, D3, 2–2 Yamadaoka, Suita, 565–0871 Japan; [*2]Department of Anatomy, Faculty of Medicine, University of Miyazaki; [*3]Department of Biofunctional Molecules, Gifu Pharmaceutical University) *A molecular chaperone inducer as potential therapeutic agent for neurodegenerative diseases*. Jpn. J. Neuropsychopharmacol., 27: 63–67 (2007).

Recent reports have shown that ER stress is involved in the pathology of some neurodegenerative diseases. In a screen for compounds that induce the ER-mediated chaperone BiP/GRP 78 (BiP), we identified BiP inducer X (BIX). BIX induced BiP only, in a dose-dependent manner, without induction of other molecules involved in the ER stress response. Pretreatment of neuroblastoma cells with BIX reduced cell death induced by ER stress. Intracerebroventricular pretreatment with BIX reduced the area of infarction due to focal cerebral ischemia in mice. In the penumbra of BIX-treated mice, ER stress-induced apoptosis was suppressed, leading to a reduction in the number of apoptotic cells. Taken together, BIX induces BiP to prevent neuronal death by ER stress, suggesting that it may be a potential therapeutic agent for cerebral diseases caused by ER stress.

**Key words:** ER stress, Molecular chaperone, Apoptosis, Cerebral ischemia, Neurodegenerative diseases

(Reprint requests should be sent to T. Kudo)

Cell Death and Differentiation (2008) 15, 364–375

www.nature.com/cdd

# A molecular chaperone inducer protects neurons from ER stress

T Kudo*,[1,6], S Kanemoto[2,3,6], H Hara[4], N Morimoto[4], T Morihara[1], R Kimura[1], T Tabira[5], K Imaizumi*,[2] and M Takeda[1]

**The endoplasmic reticulum (ER) stress response is a defense system for dealing with the accumulation of unfolded proteins in the ER lumen. Recent reports have shown that ER stress is involved in the pathology of some neurodegenerative diseases and cerebral ischemia. In a screen for compounds that induce the ER-mediated chaperone BiP (immunoglobulin heavy-chain binding protein)/GRP78 (78 kDa glucose-regulated protein), we identified BiP inducer X (BIX). BIX preferentially induced BiP with slight inductions of GRP94 (94 kDa glucose-regulated protein), calreticulin, and C/EBP homologous protein. The induction of BiP mRNA by BIX was mediated by activation of ER stress response elements upstream of the BiP gene, through the ATF6 (activating transcription factor 6) pathway. Pretreatment of neuroblastoma cells with BIX reduced cell death induced by ER stress. Intracerebroventricular pretreatment with BIX reduced the area of infarction due to focal cerebral ischemia in mice. In the penumbra of BIX-treated mice, ER stress-induced apoptosis was suppressed, leading to a reduction in the number of apoptotic cells. Considering these results together, it appears that BIX induces BiP to prevent neuronal death by ER stress, suggesting that it may be a potential therapeutic agent for cerebral diseases caused by ER stress.**
*Cell Death and Differentiation* (2008) **15,** 364–375; doi:10.1038/sj.cdd.4402276; published online 30 November 2007

The endoplasmic reticulum (ER) is an 'assembly plant' for the manufacture of secretory and membrane proteins. However, from time to time 'inferior goods', that is, unfolded/misfolded proteins in the ER are inevitable. Under normal physiological conditions, unfolded proteins are degraded; under conditions of ER stress, however, unfolded proteins can accumulate in the ER lumen. Eukaryotes utilize the unfolded protein response (UPR) to overcome the critical status induced by ER stress.[1] The UPR consists of the following three pathways: (1) suppression of protein translation to prevent the generation of more unfolded proteins; (2) facilitation of refolding of unfolded proteins by the induction of ER chaperones; and (3) activation of ER-associated degradation (ERAD) to degrade the unfolded proteins accumulated in the ER, by the ubiquitin–proteasome pathway. If these strategies are unsuccessful, cells go into ER stress-induced apoptosis.

Recent reports show that dysregulation of the UPR is implicated in much important pathology, including some neurodegenerative diseases and cerebral ischemia. Previously, the ER transducers inositol-requiring kinase 1 (IRE1), PKR(protein kinase regulated by RNA)-like ER-associated kinase (PERK), and activating transcription factor 6 (ATF6) were reported to be downregulated in presenilin-1 mutant neurons, causing the vulnerability to ER stress seen in cases of familial Alzheimer disease (AD).[2–4] Caspase 4, the human homologue of murine caspase 12, was also reported to play a critical role in ER stress-induced neuronal cell death in AD.[5] One inherited form of Parkinson's disease is associated with the accumulation of the protein Parkin-associated endothelin receptor-like receptor in the ER of dopaminergic neurons as a result of defective ERAD by mutant Parkin, a ubiquitin protein ligase (E3).[6,7] Analysis of the polyglutamine tract associated with the spinocerebrocellular atrophy protein (spinocerebellar ataxia type 3) in Machado–Joseph disease suggests that cytoplasmic accumulation of this protein can inhibit proteasome function, thereby interfering with ERAD and eliciting ER stress-induced apoptosis.[8,9] It was also reported that cerebral ischemia activates the UPR.[10,11] These findings show that many cerebral disorders are related to an impaired UPR and ER stress-induced apoptosis.

These accumulated data concerning the involvement of ER stress in cerebral disorders encouraged us to investigate this

[1]Psychiatry, Department of Integrated Medicine, Division of Internal Medicine, Osaka University Graduate School of Medicine, Suita, Japan; [2]Division of Molecular and Cellular Biology, Department of Anatomy, Faculty of Medicine, University of Miyazaki, Miyazaki, Japan; [3]Division of Structural Cellular Biology, Nara Institute of Science and Technology (NAIST) Graduate School of Biological Sciences, Ikoma, Japan; [4]Department of Biofunctional Molecules, Gifu Pharmaceutical University, Gifu, Japan and [5]National Institute for Longevity Science, Ohbu, Japan

*Corresponding authors: T Kudo, Psychiatry, Department of Integrated Medicine, Division of Internal Medicine, Osaka University Graduate School of Medicine, D3, 2-2, Yamadaoka, Suita 565-0871, Japan. Tel: +81 6 6879 3052; Fax: +81 6 6879 3059; E-mail: kudo@psy.med.osaka-u.ac.jp or
K Imaizumi, Division of Molecular and Cellular Biology, Department of Anatomy, Faculty of Medicine, University of Miyazaki, Kihara 5200, Kiyotake, Miyazaki 889-1692, Japan. Tel: +81 985 85 1783; Fax: +81 985 85 9851; E-mail: imaizumi@med.miyazaki-u.ac.jp

[6]These authors contributed equally to this work

**Keywords:** endoplasmic reticulum stress; chaperone; apoptosis; cerebral ischemia; neurodegeneration

**Abbreviations:** AD, Alzheimer disease; ATF6, activating transcription factor 6; BiP, immunoglobulin heavy-chain binding protein; CHOP, C/EBP homologous protein; EDEM, ER degradation-enhancing α-mannosidase-like protein; eIF2α, eukaryotic translation initiation factor 2 subunit α; ERAD, ER-associated degradation; ERdj4/MDG1, ER-localized DnaJ 4/microvascular differentiation gene 1; ERSE, ER stress response element; GRP78, 78 kDa glucose-regulated protein; GRP94, 94 kDa glucose-regulated protein; HSP70, 70 kDa heat-shock protein; IRE1, inositol-requiring kinase 1; MCA, middle cerebral artery; MEF, mouse embryonic fibroblast; PERK, PKR(protein kinase regulated by RNA)-like ER-associated kinase; $p58^{IPK}$, protein kinase inhibitor of 58 kDa; Tg, thapsigargin; Tm, tunicamycin; TTC, 2,3,5-triphenyltetrazolium chloride; UPR, unfolded protein response; XBP1, X-box binding protein 1

Received 02.1.07; revised 15.10.07; accepted 18.10.07; Edited by SH Kaufmann; published online 30.11.07

field in an effort to identify therapeutic targets for the treatment of these disorders. We speculate that a therapeutic strategy that induces the UPR might prevent neuronal death induced by ER stress. According to the UPR pathway, we could try to (1) induce the expression of ER molecular chaperones; (2) block translation of proteins; or (3) artificially stimulate the degradation of misfolded proteins by the proteasome, as therapeutic approaches. Indeed, some chemical compounds that induce particular UPR pathways have been developed. For example, Boyce *et al.*[12] identified salubrinal, a selective inhibitor of cellular complexes that dephosphorylates eukaryotic translation initiation factor 2 subunit $\alpha$ (eIF2$\alpha$), and thereby blocks translation. They concluded that salubrinal might be useful in the treatment of diseases involving ER stress.[12] Kim *et al.*[13] reported that valproate, a widely prescribed drug for epilepsy and bipolar disorder, increases the expression levels of the ER chaperones immunoglobulin heavy-chain binding protein (BiP), GRP94 (94 kDa glucose-regulated protein), protein disulfide isomerase, and calreticulin as well as the cytosolic chaperone HSP70 (70 kDa heat-shock protein). They also showed that valproate induces these chaperones without evoking the UPR, and speculated that inhibition of glycogen synthase kinase-3 by valproate might lead to the induction of chaperones.[13]

Previous reports have shown that induction of BiP, an ER molecular chaperone, prevents neuronal death induced by ER stress.[2,14–16] By contrast, inhibition of GRP78 (78 kDa glucose-regulated protein) mRNA induction increases cell death in response to calcium release from the ER, oxidative stress, hypoxia, and T-cell-mediated cytotoxicity.[17–19] Therefore, in this paper, we searched for a chemical compound that induces BiP for possible use as a neuroprotective agent against ER stress. We have identified such a chemical compound, BiP inducer X (BIX), and shown its protective effect against ER stress-induced apoptosis *in vivo* and *in vitro*, suggesting that this compound might be useful in the treatment of cerebral disorders associated with ER stress, such as cerebral ischemia.

## Results

**BIX preferentially induces BiP.** To identify chemical compounds that induce BiP mRNA, we utilized high-throughput screening (HTS) with a BiP reporter assay system. Of the screened compounds, 1-(3,4-dihydroxyphenyl)-2-thiocyanate-ethanone (Figure 1a) showed the highest level of induction of BiP mRNA; thus, we named this compound BiP inducer X (BIX).

First, we examined whether BIX does indeed induce the expression of BiP mRNA. Northern blot analysis and real-time PCR of SK-N-SH neuroblastoma cells treated with BIX showed that BIX induces BiP mRNA in a dose-dependent manner; however, the level of BiP mRNA induced by BIX is less than that induced by thapsigargin (Tg) (Figure 1b). Additionally, treatment of cells with 50 $\mu$M BIX caused the highest induction of BiP and little toxicity to cells. Because BIX generated cytotoxicity at higher dosages, we did not use it at concentrations greater than 50 $\mu$M in further analyses. Semiquantitative RT-PCR and real-time PCR showed that the BiP signal peaked at 4 h after the addition of 5 $\mu$M BIX and remained at that level until 6 h after treatment, with a subsequent reduction in level after this point (Figure 1c). To determine whether the induction of BiP mRNA by BIX results in an increase in the level of BiP protein, we carried out immunoblot analysis. As shown in Figure 1d, the level of BiP protein was increased by 5 $\mu$M BIX in a time-dependent manner, consistent with the changes in mRNA levels.

Next, we performed semiquantitative RT-PCR analysis to investigate whether BIX affects the expression of any other ER stress response-related genes, such as GRP94, calreticulin, X-box binding protein 1 (XBP1), ER-localized DnaJ 4/microvascular differentiation gene 1 (ERdj4/MDG1), ER degradation-enhancing $\alpha$-mannosidase-like protein (EDEM), protein kinase inhibitor of 58 kDa ($p58^{IPK}$), C/EBP homologous protein (CHOP), and asparagine synthetase (ASNS) (Figure 2a). According to the time-course study of BiP induction by BIX (Figure 1c), a 6 h treatment of cells with BIX was adopted into this study. XBP1 mRNA, which is spliced under ER stress induced by 1 $\mu$M Tg or 1 $\mu$g/ml tunicamycin (Tm), was not processed in cells treated with 5 $\mu$M BIX. Compared with a control sample, ERdj4/MDG1, EDEM, $p58^{IPK}$, and ASNS were scarcely induced by BIX. On the other hand, GRP94, calreticulin, and CHOP were induced by BIX, but their inductions were not as prominent as that of BiP. We also performed time-course analyses on the expressions of ER stress response-related genes by real-time PCR in SK-N-SH cells treated with 50 $\mu$M BIX as well as 5 $\mu$M BIX. A 5 $\mu$M portion of BIX induced GRP94, calreticulin, and CHOP mRNA as well as BiP. However, BiP was definitely induced from 2 to 6 h (Figure 2b). The time courses for EDEM, $p58^{IPK}$, and ASNS were not changed by treatment with 5 $\mu$M BIX (Figure 2b). A 50 $\mu$M portion of BIX also induced BiP from 4 to 6 h and transiently induced calreticulin and CHOP. Even 50 $\mu$M BIX did not induce EDEM, $p58^{IPK}$, or ASNS (Figure 2b).

Moreover, we performed immunoblot analysis of GRP94 and phosphorylated eIF2$\alpha$ to examine whether BIX affects other signaling pathways that participate in the ER stress response. Treatment of SK-N-SH cells with BIX caused very slight induction of GRP94 protein compared with its induction by 1 $\mu$M Tg (Figure 2c). This result was consistent with that of semiquantitative RT-PCR analysis of the GRP94 mRNA level. Treatment of cells with 1 $\mu$M Tg increased the level of phosphorylated eIF2$\alpha$, but BIX did not cause its phosphorylation (Figure 2c). These results indicate that BIX invokes little ER stress, but almost preferentially induces BiP.

**The induction of BiP by BIX is mediated by activation of ERSEs through the ATF6 pathway.** To investigate the mechanism by which BiP is induced by BIX, we performed reporter assays using 132 bp BiP-pGL3 reporter plasmids as described in the Materials and Methods section. A BiP (132)-pGL3 plasmid (Figure 3a) was transfected into SK-N-SH cells and the cells were treated with 5 $\mu$M BIX, 300 nM Tg, or 0.5 $\mu$g/ml Tm for either 6 or 16 h. The reporter activities in transfectants were elevated in response to stimulation with Tg or Tm, and maintained at a long-lasting high level (Figure 3b). By contrast, reporter activities in cells treated with BIX were transiently induced at 6 h after stimulation and then downregulated to basal levels by 16 h (Figure 3b). This

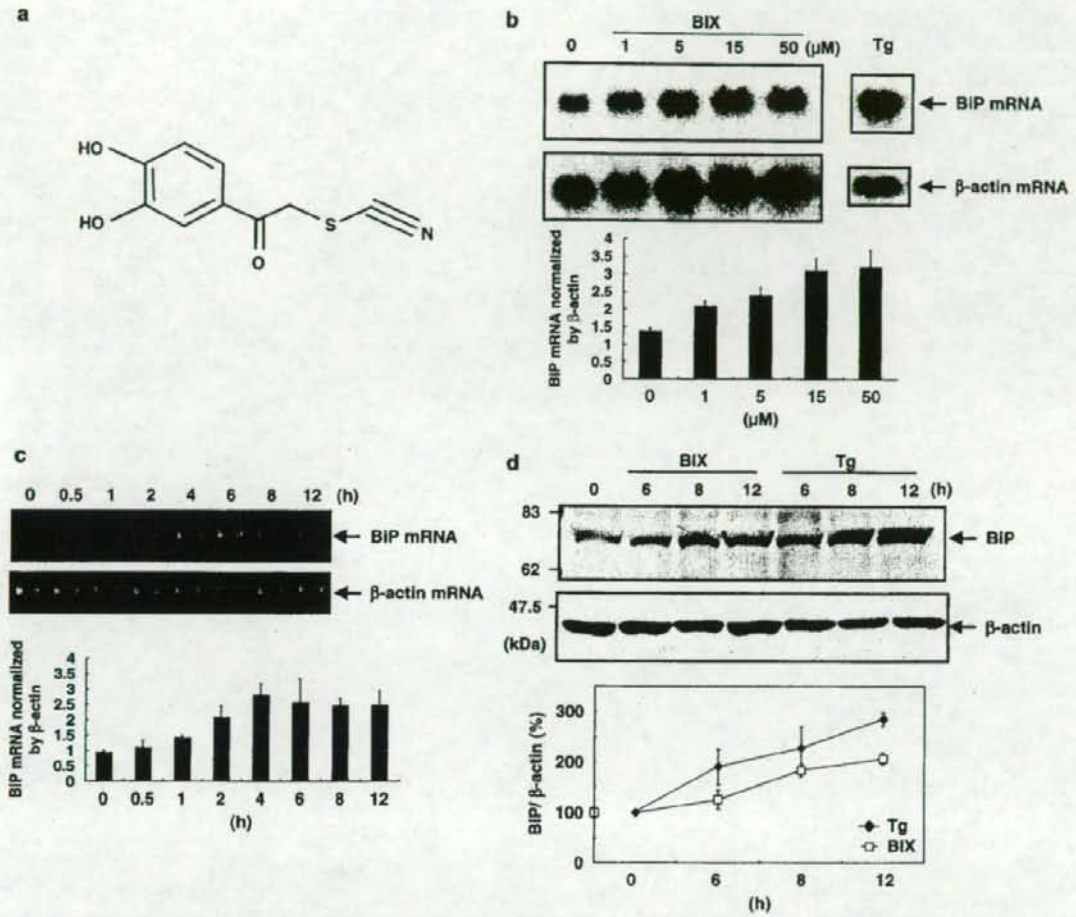


**Figure 1** BIX induces BiP. (**a**) The structure of BIX (1-(3,4-dihydroxyphenyl)-2-thiocyanate-ethanone). (**b**) Dose-dependent induction of BiP mRNA in SK-N-SH cells after 6 h of treatment with BIX is shown by northern blot (upper panel) and real-time PCR (lower panel); values are means ± S.D. from three independent experiments. The induction of BiP mRNA by Tg is shown as a positive control. $\beta$-Actin mRNA is shown as an internal control. (**c**) The time course of BiP mRNA induction in cells treated with BIX is shown by semiquantitative RT-PCR (upper panel) and real-time PCR (lower panel); values are means ± S.D. from three independent experiments. The level of BiP mRNA peaked in 4 h and kept until 6 h after treatment with BIX at 5 $\mu$M, with a subsequent reduction after this point. (**d**) A time-dependent induction of BiP protein in SK-N-SH cells treated with 5 $\mu$M BIX or 1 $\mu$M Tg is detected by immunoblot and quantified by densitometry. Values are means ± S.D. from three independent experiments

finding supports the results shown in Figure 1c and suggests that the effects of BIX on BiP induction are transient and that BiP mRNA reverts to basal levels. Therefore, induction of BiP by BIX might be caused by a mechanism different to that used by ER stressors such as Tg and Tm, and the BIX-responsive element(s) might be included in the 132 bp BiP promoter region. Within this 132 bp region, there are three ER stress response elements (ERSEs) (Figure 3a). Subsequently, we carried out the reporter assay using an ERSE mut (132)-pGL3 plasmid (Figure 3a) to confirm whether or not these ERSEs are involved in the induction of BiP by BIX. BiP (132)-pGL3 or ERSE mut (132)-pGL3 was transfected into SK-N-SH cells, and the cells were treated with 5 $\mu$M BIX for 6 h. The reporter activities in cells transfected with BiP (132)-pGL3 were increased ~4-fold by BIX. On the other hand, induction of reporter activity was not observed in cells transfected with ERSE mut (132)-pGL3 (Figure 3c). This result suggests that ERSEs are involved in the induction of BiP by BIX.

Next, to examine whether three major transducers of the ER stress response, namely PERK, IRE1, and ATF6, affect the induction of BiP by BIX, we analyzed the expression of BiP in knockout/knockdown mouse embryonic fibroblasts (MEFs) lacking each transducer (Figure 3d). In PERK-deficient MEFs and IRE1$\alpha/\beta$ double-knockout MEFs, BiP mRNA was induced by BIX to a similar level to that seen in wild-type cells

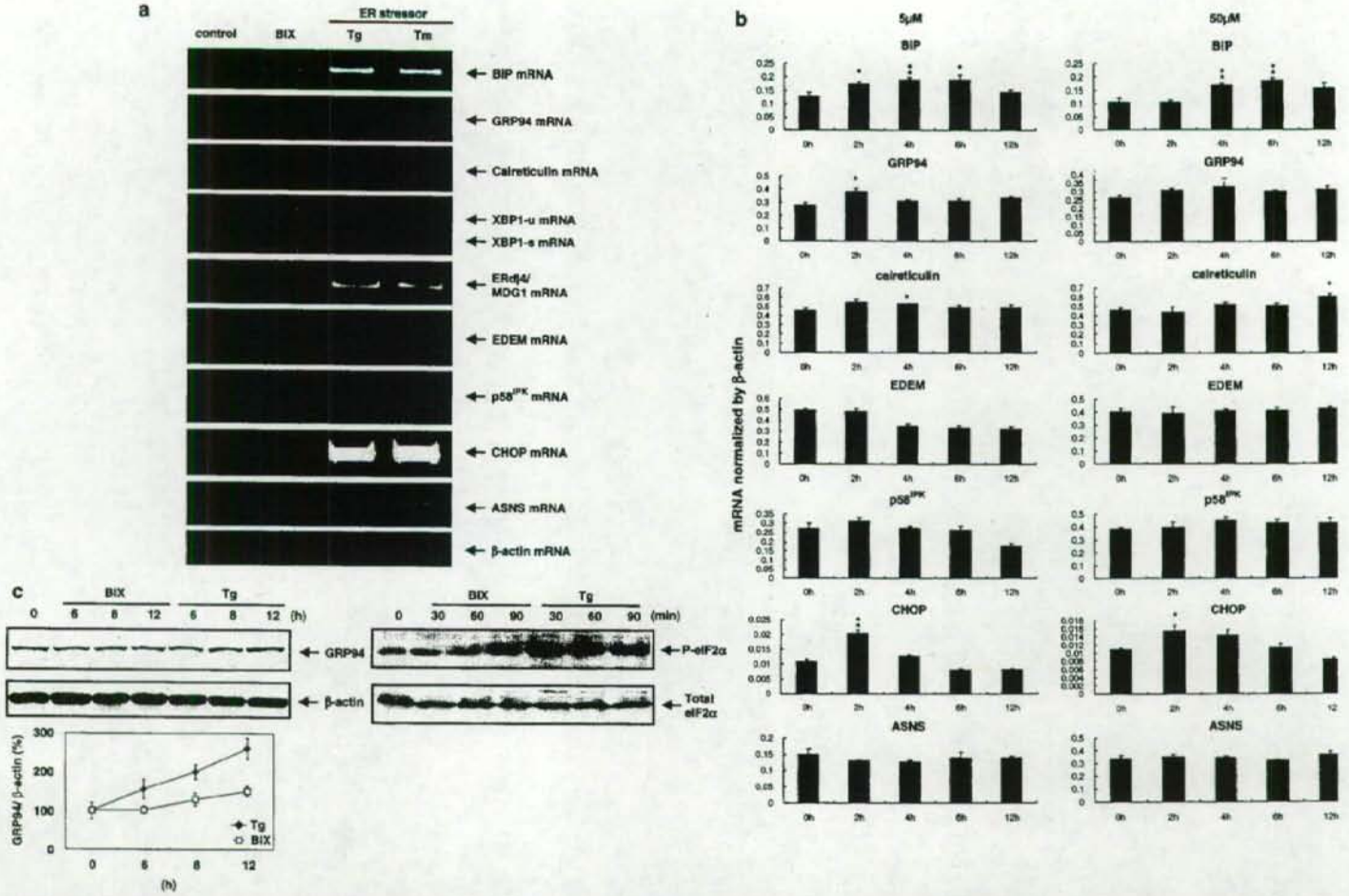


**Figure 2** BIX preferentially induces BiP. (a) Semiquantitative RT-PCR analysis shows that a 6 h treatment of cells with 5 $\mu$M BIX induces BiP mRNA but not spliced XBP1 (XBP1-s), ERdj4/MDG1, EDEM, p58$^{IPK}$, and ASNS mRNAs, which are induced by 1 $\mu$M Tg or 1 $\mu$g/ml Tm. GRP94, calreticulin, CHOP are slightly induced by BIX. (b) Time-course analyses by real-time PCR show that 5 $\mu$M BIX significantly induces BiP from 2 to 6 h after BIX administration and transiently induces GRP94, calreticulin, and CHOP. The mRNAs of EDEM, p58$^{IPK}$, and ASNS are not changed from 2 to 12 h. A 50 $\mu$M portion of BIX also induces BiP from 4 to 6 h and transiently induces calreticulin and CHOP. Even 50 $\mu$M BIX does not induce EDEM, p58$^{IPK}$, and ASNS. Values are means ± S.E. from 3–4 independent experiments. Significant differences are based on the values at 0 h, $^{*}P<0.05$, $^{**}P<0.01$. (c) Immunoblot analysis with quantification shows that 5 $\mu$M BIX causes very slight induction of GRP94 protein but does not induce the phosphorylation of eIF2$\alpha$ at any time point, compared with 1 $\mu$M Tg. Values are means ± S.D. from three independent experiments

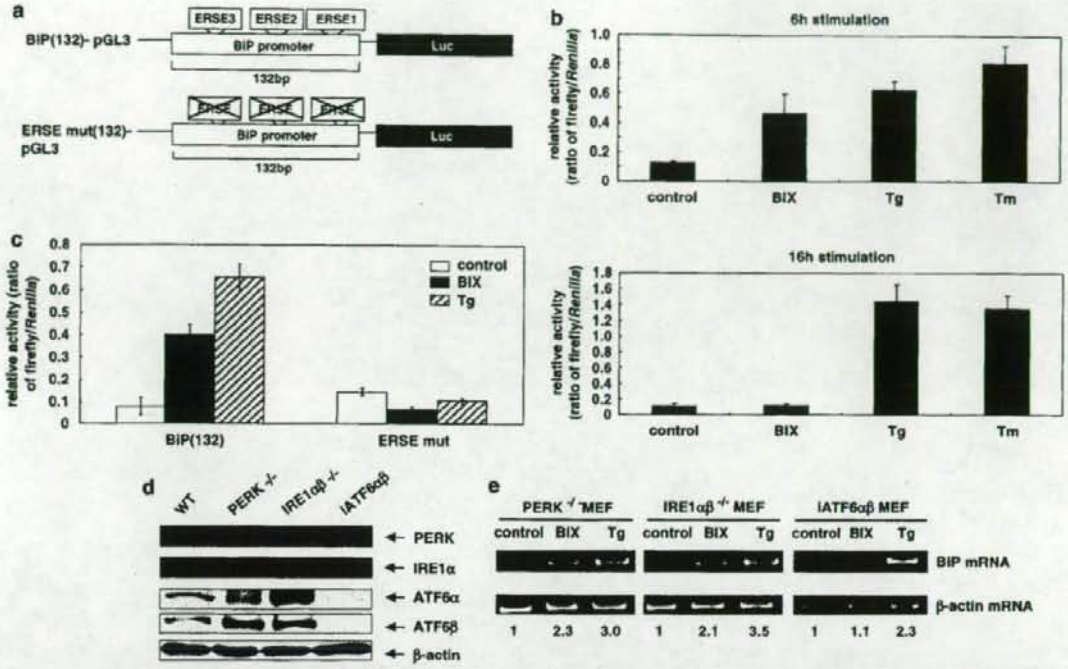


**Figure 3** The induction of BiP by BIX is mediated by ERSE and the ATF6 pathway. (**a**) Schematic representation of the BiP promoter cloned into the pGL3 plasmid (BiP (132)-pGL3) and the ERSE mutant BiP promoter cloned into the pGL3 plasmid (ERSE mut (132)-pGL3). (**b**) The luciferase activities driven by the BiP promoter are normalized against *Renilla* luciferase activities. The induction of luciferase activity in BiP (132)-pGL3-transfected cells that are treated with 5 $\mu$M BIX increased at 6 h after BIX treatment and reversed to basal levels by 16 h. Induction of luciferase activity in 300 nM Tg- or 0.5 $\mu$g/ml Tm-treated cells is sustained until 16 h after BIX treatment. Values are means ± S.D. from five independent experiments. (**c**) The relative reporter activity in cells transfected with BiP (132)-pGL3 (ratio of firefly/*Renilla*) at 6 h after treatment in cells treated with BIX (5 $\mu$M) are increased ~4-fold, whereas that in cells transfected with ERSE mut (132)-pGL3 are not increased. Values are means ± S.D. from five independent experiments. Tg (300 nM) also increases reporter activity in cells transfected with BiP (132)-pGL3, but not in cells transfected with mut (132)-pGL3. (**d**) Immunoblot analyses of PERK$^{-/-}$ MEFs, IRE1$\alpha\beta^{-/-}$ MEFs, and iATF6$\alpha\beta$ (knockdown) MEFs with anti-PERK, anti-IRE1 and anti-ATF6$\alpha/\beta$ antibodies prove the deficiency of those genes. (**e**) Semiquantitative RT-PCR analysis shows that BiP mRNA is induced at 6 h after treatment with BIX (50 $\mu$M) in PERK$^{-/-}$ MEFs and IRE1$\alpha\beta^{-/-}$ MEFs, but not in iATF6$\alpha\beta$ (knockdown) MEFs. Tg induces BiP mRNA in all three MEFs. Numeric values below the panels indicate the induction ratio of BiP mRNA adjusted to the level of $\beta$-actin mRNA with reference to non-treated control sample as one

(Figure 3e). These results indicate that the induction of BiP by BIX is not mediated via the PERK or IRE1 pathways. The data showing that eIF2$\alpha$ is not phosphorylated by BIX (Figure 2c), and that XBP1 is not processed by BIX (Figure 2a), support this conclusion. By contrast, BiP was not induced by BIX in ATF6$\alpha\beta$ double-knockdown MEFs (Figure 3e), suggesting that BIX treatment mediates the induction of BiP via the ATF6 pathway. These results were also obtained by northern blot analysis (data not shown). The data showing that BIX induced GRP94, calreticulin, and CHOP, and that ERdj4/MDG1, EDEM, p58$^{IPK}$ and ASNS were not induced by BIX (Figure 2a, b), also suggested that the effect of BIX is mediated by the ATF6 pathway. This is because the inductions of GRP94, calreticulin, and CHOP are known to be dependent on the activation of ATF6; inductions of ERdj4/MDG1, EDEM, p58$^{IPK}$ are known to be mediated by IRE1 and that of ASNS by PERK. Next, we tried to detect the cleavage of ATF6 in cells treated with BIX, but we have not yet detected cleaved N-terminal fragments of endogenous ATF6 using the antibody described in this study (data not shown).

**BIX protects SK-N-SH cells from ER stress-induced apoptosis.** BiP functions as a cytoprotective protein in stressed cells.[14–16] As BIX activates BiP expression, BIX might protect cells from ER stress. To investigate whether BIX has the ability to prevent apoptosis induced by ER stress, SK-N-SH cells were pretreated for 12 h with 0 or 5 $\mu$M BIX, which was then replaced with fresh medium containing 0.5 $\mu$g/ml Tm. Phase-contrast images (Figure 4a–d) and fluorescence micrographs (Figure 4e–h) of Hoechst staining show that apoptotic cell death was observed within 36 h of Tm treatment (Figure 4d, h), and that the number of dead cells had increased significantly (Figure 4i). By contrast, cell death was significantly inhibited by pretreatment with BIX (Figure 4c, g, i). We also found that treatment of cells with BIX only for 36 h caused no changes in cells (Figure 4b, f). Next, we looked at the activation of caspases 4 and 3/7 after ER stress. Caspase 4 was reported to be activated in response to ER stress in human cells.[5] Immunoblot analysis showed that pretreatment of cells with BIX attenuated the cleavage of caspase 4 (Figure 4j). Moreover, we analyzed

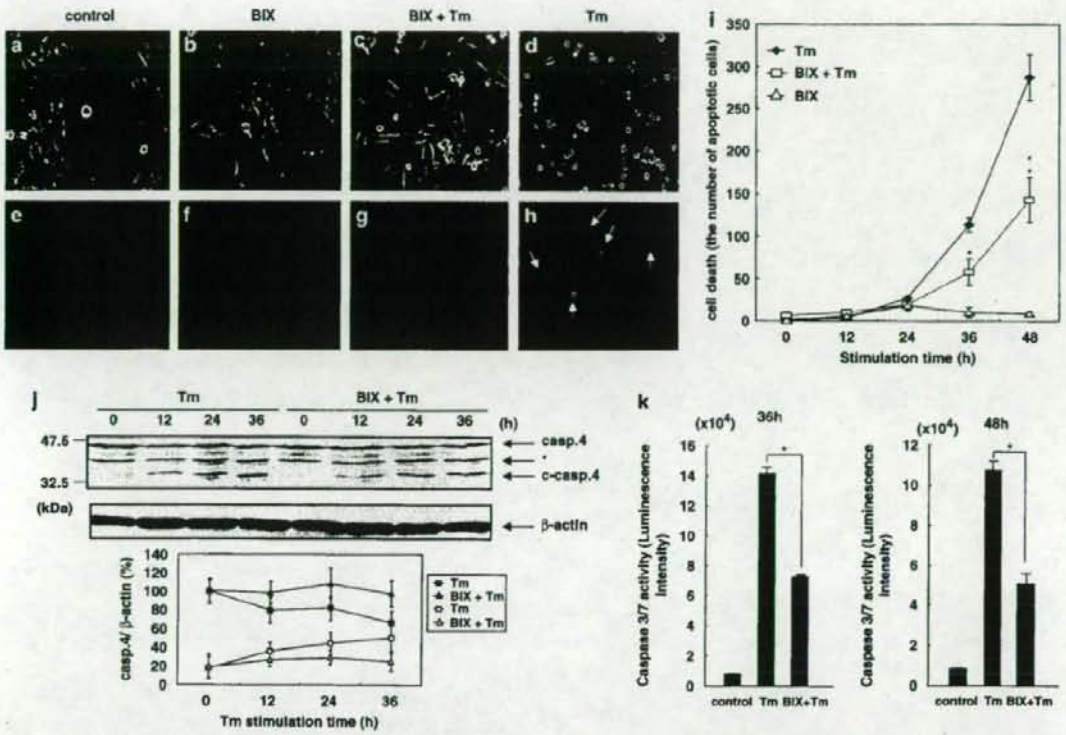


**Figure 4** BIX protects SK-N-SH cells from ER stress-induced apoptosis. SK-N-SH cells are pretreated with vehicle (control: **a**, **e**; Tm: **d**, **h**) or with 5 $\mu$M BIX (BIX: **b**, **f**; BIX + Tm: **c**, **g**) for 12 h, and then the whole medium is replaced with fresh medium (control, BIX) or medium supplemented with 0.5 $\mu$g/ml Tm (BIX + Tm, Tm). Phase-contrast images (**a**–**d**) and fluorescence micrographs of Hoechst staining (**e**–**h**) at 36 h after Tm stimulation show that pretreatment of cells with BIX reduces the number of Tm-induced apoptotic cells. Arrows show apoptotic cells (h). (**i**) The number of dead cells (apoptotic cells) after Tm treatment increases from 0 to 48 h. Pretreatment of cells with BIX significantly reduces the amount of cell death compared with cells treated with Tm only (*$P<0.05$, **$P<0.01$). BIX alone does not cause remarkable cell death. A total of 500 cells are counted at each time point. Values are means ± S.D. from five independent experiments. (**j**) Immunoblot of caspase 4 shows that Tm causes cleavage of caspase 4 (c-Casp.4) in a time-dependent manner and that pretreatment of cells with BIX attenuates this cleavage with no change in the level of $\beta$-actin. Asterisk indicates nonspecific bands. The lower panel shows quantitative analyses of full-length and cleaved caspase 4. Filled square and triangle indicate full-length caspase 4; open square and triangle indicate cleaved caspase 4. Values are means ± S.D. from three independent experiments. (**k**) The caspases 3 and 7 activities in Tm-treated cells are increased. BIX reduces this caspase activity to almost half value of the Tm-treated levels. Values are means ± S.D. from three independent experiments; *$P<0.01$

the activities of caspases 3 and 7. The activities of caspases 3 and 7 in Tm-treated cells were extremely high. By contrast, BIX reduced the activities of caspases 3 and 7 to half of those in cells treated with Tm only (Figure 4k). Taken together, these findings suggest that pretreatment of cells with BIX inhibits cell death induced by ER stress involving inhibited activation of caspases 3/7 and 4.

**BIX administration reduces the insults due to cerebral infarction.** Because it has been shown that cerebral ischemia causes ER stress,[20] we performed occlusions of the middle cerebral arteries (MCAs) of mice to confirm whether the protective effects of BIX *in vitro* can be utilized *in vivo*. Immunoblot analysis of extracts from the cerebral hemisphere showed that 20 $\mu$g (2 $\mu$l) of BIX (administered intracerebroventricularly) significantly increased the level of BiP protein 24 h after administration, confirming that administration of BIX induces BiP protein *in vivo* (Figure 5a). Real-time PCR analysis of the expression of ER stress response-related genes showed that 20 $\mu$g BIX significantly induced BiP at 6 h after administration (Figure 5b). The levels of GRP94, calreticulin, and CHOP mRNA also increased; however, those of EDEM, p58$^{IPK}$, and ASNS did not change (Figure 5b), consistent with the results of *in vitro* study (Figure 2b). Animals treated with BIX showed no behavioral changes, except for the neurological deficits induced by ischemia. Neurological evaluation at 24 h after MCA occlusion showed that most of the vehicle-administered (control) mice presented with moderate symptoms; for example, circling to the contralateral side (Figure 5c). By contrast, most BIX-administered (5 or 20 $\mu$g) mice presented with milder symptoms; for example, extending the right forepaw (Figure 5c).

Twenty-four hours after occlusion, 2,3,5-triphenyltetrazolium chloride (TTC) staining showed that the mice had developed infarcts affecting the ipsilateral cortex and striatum

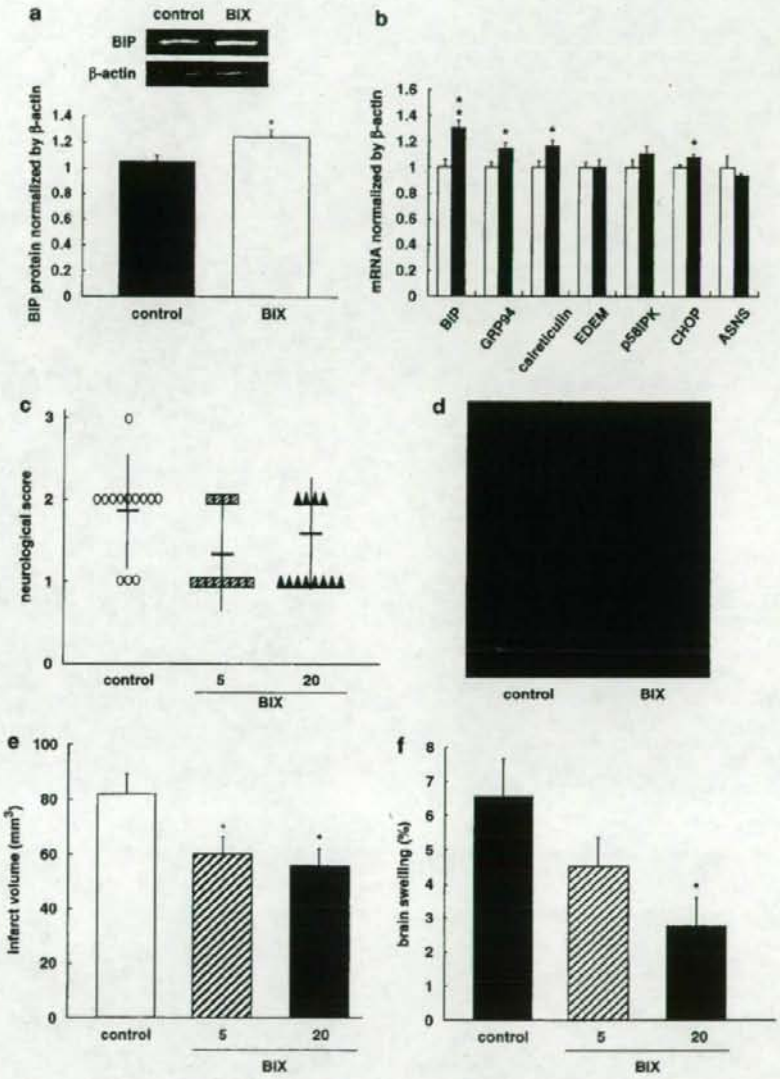


**Figure 5** BIX administration reduces the extent of cerebral infarction after MCA occlusion. (**a**) It is confirmed that intracerebroventricular administration of BIX raises the level of BiP protein in mouse brains. Immunoblot analysis of BiP and $\beta$-actin protein in BIX-administered (20 $\mu$g/2 $\mu$l) brains shows that the level of BiP protein is significantly increased at 24 h after BIX administration compared with vehicle-treated brains. The inset is the representative immunoblot detected by luminescence of ECL. Densitometric scanning of BiP bands normalized to $\beta$-actin was performed. Data are represented as means ± S.E. from four independent experiments; $^{*}P<0.05$. (**b**) The real-time PCR shows that the level of BiP (in arbitrary units) in the BIX-administered (20 $\mu$g/2 $\mu$l) hemisphere is increased significantly at 6 h after administration. The levels of GRP94, calreticulin, and CHOP mRNA are increased by BIX, the levels of EDEM, p58$^{IPK}$, and ASNS do not change. The black bar is the BIX-administered (20 $\mu$g/2 $\mu$l) hemisphere; the white bar is the vehicle-administered hemisphere. Values are means ± S.E. from 3–4 independent experiments; $^{*}P<0.05$, $^{**}P<0.01$. (**c**) Neurological deficits at 24 h after occlusion of the MCA are scored using the following scale: 0 = no observable neurological deficits (normal); 1 = failure to extend the right forepaw (mild); 2 = circling to the contralateral side (moderate); 3 = loss of walking or righting reflex (severe). BIX administration (5 or 20 $\mu$g) improves neurological deficits induced by MCA occlusion. Values are means (horizontal bold bar) ± S.D. (**d**) Representative images of TTC staining at 24 h after MCA occlusion. Note that the infarct area (white or pink) in BIX-administered brains is smaller than that in brains treated with vehicle. (**e**) Quantitative analysis of infarct volumes measured by TTC staining. Values are means ± S.E. from 12 or 13 independent experiments; $^{*}P<0.05$. (**f**) BIX administration (5 or 20 $\mu$g) reduces brain swelling induced by MCA occlusion. Values are means ± S.E. from 12 or 13 independent experiments; $^{*}P<0.05$

(Figure 5d). The core of infarction was observed as a white area and the penumbra was pink. The infarction area (core + penumbra) observed in BIX-treated brains was smaller than that in vehicle-treated brains (Figure 5d). Quantitation of TTC staining showed that administration of 5 or 20 $\mu$g of BIX significantly reduced the infarction area (Figure 5e). Furthermore, measurement of brain swelling also showed that administration of 20 $\mu$g of BIX significantly reduced brain swelling after 24 h of ischemia (Figure 5f).

**BIX administration reduces apoptosis induced in the penumbra by MCA occlusion.** Detailed observation of TTC-stained ischemic brains indicated that the reduction in the area of infarction in BIX-treated brains was predominantly due to a reduction in the area of the penumbra rather than the core. Therefore, we examined the penumbra of BIX-treated brain for evidence of apoptosis. Terminal deoxynucleotidyl transferase-mediated dUTP–biotin nick end labeling (TUNEL) staining of ischemic brains without BIX treatment revealed an increased number of TUNEL-positive cells in the ipsilateral core and penumbra compared with the contralateral side (Figure 6a). By contrast, the number of TUNEL-positive cells was significantly reduced in the ipsilateral penumbra of BIX-treated brains compared with that of vehicle-treated brains (Figure 6a, b). Immunohistochemistry for caspase 3 in the penumbrae of BIX- and vehicle-treated brains showed that BIX reduced the number of apoptotic cells at 24 h after MCA occlusion (Figure 6c, d). CHOP plays a role in apoptotic cell death by ER stress.[21] Moreover, it is well-known that CHOP is induced after ischemic insults.[22] Therefore, we examined the effects of BIX treatment on the induction of CHOP mRNA after ischemia. *In situ* hybridization analysis showed that CHOP mRNA was significantly induced in the penumbra of MCA-occluded mice, whereas pretreatment of mice with BIX resulted in a marked reduction in the level of CHOP mRNA expression (Figure 6e, f). Although BIX induced CHOP (Figure 5b), the extent of this induction was very weak compared with the expression induced by ischemia (Figure 6e, f). The results of TUNEL staining and *in situ* hybridization for CHOP indicate that BIX suppresses the ER stress-mediated apoptotic cell death induced in the penumbra after ischemia.

## Discussion

If a BiP inducer is just an ER stressor such as Tg or Tm, its application as a therapeutic strategy is unlikely to be realized because it may activate several pathways of the UPR, including ER stress-induced apoptotic pathways. The present studies in knockout or knockdown MEFs deficient in ER stress sensors showed that the ATF6 pathway is necessary for BIX to induce BiP. This is consistent with the evidence that BIX preferentially induced BiP with slight inductions of GRP94, calreticulin, and CHOP mediated by the ATF6 pathway, and that BIX does not affect the pathway downstream of IRE1 or the translational control branch downstream of PERK. Moreover, for the apoptotic branches of ER stress, the transient induction of CHOP by BIX was very weak compared with the severe induction observed in ER stress, and caspase 4 was not activated by BIX. The differences among inductions between BiP and the other genes of the ATF6 pathway by BIX suggested that elements other than ERSEs may be involved in the induction of BiP by BIX.

The present data from *in vitro* studies showed that BIX suppresses the cleavage of caspase 4, a member of one of the apoptotic pathways mediated by ER stress. Because it was reported that PERK is activated after cerebral ischemia[10] and that XBP1 mRNA splicing is detected after transient cerebral ischemia,[11] it would appear that cerebral ischemia causes ER stress. Thus, to examine the antiapoptotic effect of BIX *in vivo*, we used MCA-occluded mice. Intracerebroventricular pretreatment of mice with BIX reduced the area of infarction in the brain, especially the area of the penumbra. BIX pretreatment also reduced the severity of neurological deficits caused by focal cerebral ischemia. In the penumbrae of BIX-treated brains, the induction of CHOP, an apoptotic molecule induced by ER stress, was suppressed, suggesting that BIX reduces cell death by preventing ER stress-induced apoptosis. As the infarct volumes, brain swelling, and neurological scores following 5 and 20 $\mu$g treatments were similar, 5 $\mu$g of BIX might be sufficient to protect against ischemia. This is the first report demonstrating the *in vivo* success of a therapeutic manipulation to inhibit apoptosis mediated by ER stress, indicting that BIX might be a potential therapeutic for neuroprotection after cerebral infarction.

The induction of BiP by BIX was transient, peaking at 4 h after treatment, but the levels of BiP protein continued to increase until 12 h. The reporter assay using the 132 bp BiP-pGL3 plasmid also showed that the effect of BIX on the induction of BiP was transient and weaker than the effect of ER stressors, such as Tg or Tm. Even a high dosage of BIX (50 $\mu$M) did not induce genes mediated by non-ATF6 pathways. These results imply that the mechanism of BiP induction utilized by BIX may be different from those used by these ER stressors. It was reported that the activation of transducers of ER stress is caused by dissociation of BiP from their luminal domains.[23] It may be assumed that artificial induction of BiP disturbs the activation of transducers of ER stress, because abundant BiP remains bound to these transducers preventing their activation. However, the effect of BIX peaked at 4 h and remained at that level until 6 h after treatment; after this point, there was a subsequent reduction in level. Therefore, the production of BiP induced by BIX may not disturb this dissociation.

An earlier study showed that a selective inhibitor of eIF2$\alpha$ dephosphorylation protects cells from ER stress[12] and that the development of novel chemical compounds for diseases related to ER stress is underway. It is possible that BIX, which has effects *in vivo*, could have therapeutic applications in the treatment of diseases involving ER stress. We propose that BiP activators, such as BIX, will be effective agents against ER stress. However, further studies will be required to investigate the pharmacology of BIX, including its possible side effects, before BiP activators can be used in clinical practice.

## Materials and Methods

**Cell culture.** SK-N-SH neuroblastoma cells were grown in $\alpha$-modified Eagle's medium supplemented with 10% fetal bovine serum. MEFs derived from IRE1$^{-/-}$ embryos or PERK$^{-/-}$ embryos were cultured in Dulbecco's modified Eagle's

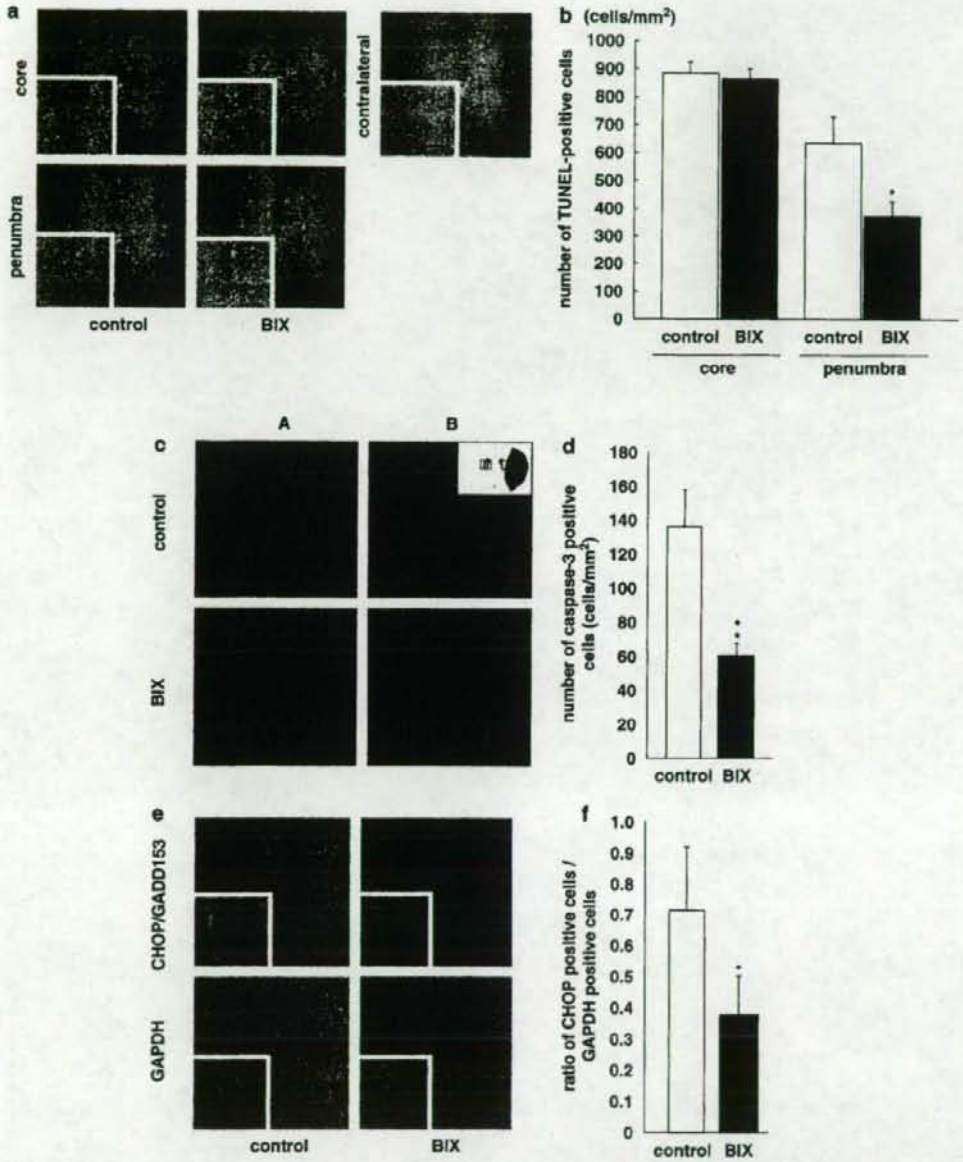


**Figure 6** A 20 $\mu$g portion of BIX administration reduces ER stress-induced apoptosis induced in the penumbra by MCA occlusion. (**a**) Representative images of TUNEL staining in the core, penumbra, or contralateral side to the infarction at 24 h. Insets are higher magnification images. BIX administration reduces the number of TUNEL-positive cells induced in the penumbra by MCA occlusion. Scale bar for higher magnification panels, 10 $\mu$m; lower magnification panels, 100 $\mu$m. (**b**) Cell-counting analysis shows that BIX significantly reduced the number of TUNEL-positive cells in the penumbra. Values are means ± S.D. from 9 or 10 independent experiments; $^{*}P<0.05$. (**c**) Representative image showing immunohistochemical staining for caspase 3 in the penumbra area (**A**) and contralateral area (**B**) in a BIX-treated mouse and vehicle-treated mouse at 24 h after treatment. Scale bar, 50 $\mu$m. (**d**) Quantitative analysis of caspase 3-positive cells. Values shown are the number of caspase 3-positive cells/mm$^2$. Values are means ± S.D. from five independent experiments; $^{**}P<0.01$. (**e**) Representative images of *in situ* hybridization for CHOP, an apoptotic molecule induced in penumbra by ER stress at 24 h. Insets are higher magnification images. Scale bar for higher magnification panels, 10 $\mu$m; lower magnification panels, 100 $\mu$m. (**f**) Quantitative analysis of CHOP-positive cells. Values shown are the ratios of CHOP-/GAPDH-positive cells. Values are means ± S.D. from five independent experiments; $^{*}P<0.05$

medium supplemented with 10% fetal bovine serum. MEFs in which both ATF6α and ATF6β (iATF6αβMEF) had been knocked down were also maintained in the Dulbecco's modified Eagle's medium. PERK$^{-/-}$ MEFs, IRE1$^{-/-}$ MEFs, and iATF6αβMEFs were kindly provided by Drs. David Ron (New York University, NY, USA), Dr. Fumihiko Urano (University of Massachusetts Medical School, MA, USA), and Laurie H Glimcher (Harvard School of Public Health, MA, USA), respectively.

**Reagents.** Cells were treated with Tm or Tg to induce ER stress conditions. Tm was purchased from Sigma (St. Louis, MO, USA). Tg was purchased from Alomone Labs Ltd (Jerusalem, Israel). Hoechst staining was performed according to the manufacturer's instructions.

**Plasmids.** A pGL3-BiP promoter (132)-Luc reporter plasmid (BiP (132)-pGL3) and an ERSE mutant BiP promoter-Luc reporter plasmid (ERSE mut (132)-pGL3) were provided by Dr. K Mori (Kyoto University, Kyoto, Japan).

**Transfection and reporter assays.** SK-N-SH cells were grown to 80% confluence and then transfected using Lipofectamine 2000 reagent, according to the manufacturer's instructions (Invitrogen, Carlsbad, CA, USA). Cells were transfected with a reporter plasmid (0.2 μg) carrying the firefly luciferase gene under the control of the BiP promoter, and a reference plasmid pRL-SV40 (0.02 μg) carrying the *Renilla* luciferase gene under the control of the SV40 enhancer and promoter (Promega, Madison, WI, USA). At 12 h after transfection, cells were treated with library compounds to screen for compounds that induce BiP. Firefly and *Renilla* luciferase activities were measured in 10 μl of cell lysate using a Dual-Luciferase Reporter Assay System (Promega) and a luminometer (Berthold Technologies, Bad Wildbad, Germany). Relative luciferase activity was defined as the ratio of firefly luciferase activity to *Renilla* luciferase activity. Values were averaged from quadruplicate determinations. Using these BiP reporter cells, HTS was performed on a compound library consisting of approximately 10 000 compounds. The molecules were synthesized based on the structures of 10 lead compounds that had high activity in HTS. Among the synthesized molecules, we chose a small molecule that had the highest activity, naming it BIX. To confirm the induction of BiP by this compound, 5 μM BIX, 300 nM Tg or 0.5 μg/ml Tm were added to cell and the luciferase assay was performed as described; luciferase activities were measured in three independent experiments.

**RNA isolation and semiquantitative RT-PCR analysis.** SK-N-SH cells or MEFs were washed with phosphate-buffered saline (PBS) and then collected by centrifugation. Total RNA was isolated from cells using an RNeasy kit (Qiagen, Tokyo, Japan) according to the manufacturer's protocol. Total RNA was isolated from frozen brains using the acid guanidine–phenol–chloroform RNA extraction method provided as ISOGEN (Nippon Gene, Toyama, Japan), and purified using an RNeasy Mini kit (Qiagen). RNA concentrations were determined spectrophotometrically at 260 nm. First-strand cDNA was synthesized in a 20-μl reaction volume using a random primer (Takara, Shiga, Japan) and Moloney murine leukemia virus reverse transcriptase (Invitrogen). PCR was performed in a total volume of 30 μl containing 0.8 μM of each primer, 0.2 mM dNTPs, 3 U *Taq* DNA polymerase (Promega), 2.5 mM $MgCl_2$, and 1 × PCR buffer. The amplification conditions for semiquantitative RT-PCR analysis were as follows: an initial denaturation step of 95°C for 5 min, 22 cycles of 95°C for 1 min, 55°C for 1 min, and 72°C for 1 min, and a final extension step of 72°C for 7 min. The numbers of amplification cycles for detection of BiP and β-actin were 18 and 15, respectively. The primers used for amplification were as follows: BiP: 5′-GTTTGCTGAGGAAGACAAAAAGCTC-3′ and 5′-CACTTCCATAGAGTTTGCTGATAATTG-3′; XBP1: 5′-CAGCGCTTGGGGATGGATGC-3′ and 5′-CCATGGGGAGATGTTCTGGA-3′; CHOP: 5′-GGAGCTGGAAGCCTGGTATGAGG-3′ and 5′-TCCCTGGTCAGGCGCTCGATTTCC-3′; GRP94: 5′- CTCACCATTTGGATCCTGTGTG-3′ and 5′-CACATGACAAGATTTTACATCAAGA-3′; calreticulin: 5′-GCCAAGGACGAGCTGTAGAGAG-3′ and 5′-GGTGAGGGCTGAAGGAGAATC-3′; ERdj4/MDG1: 5′-TCTAGAATGGCTACTCCCCAGTCAATTTTC-3′ and 5′-TCTAGACTACTGTCCTGAACAGTCAGTG-3′; EDEM: 5′-TGGGTTGGAAAGCAGAGTGGC-3′ and 5′-TCCATTCCTACATGGAGGTAG-3′; $p58^{IPK}$ 5′-GAGGTTTGTGTTTGGGATGCAG-3′ and 5′-GCTCTTCAGCTGACTCAATCAG-3′; ASNS: 5′-AGGTTGATGATGCAATGATGG-3′ and 5′-TCCCCTATCTACCCACAGTCC-3′; β-actin: 5′-TCCTCCCTGGAGAAGAGCTAC-3′ and 5′-TCCTGCTTGCTGATCCACAT-3′. PCR products were resolved by electrophoresis through 4.8% (w/v) polyacrylamide gels. The density of each band was quantified using the Scion Image Program (Scion Corporation, Frederick, MD, USA).

**Northern blot analysis.** Total RNA (10 μg/lane) was resolved by electrophoresis through 1.0% agarose/formaldehyde gels and transferred onto Immobilon-NY + membranes (Millipore, Bedford, MA, USA). Filters were hybridized with $^{32}$P-labeled cDNA probes generated from the BiP cDNA by the Random Primer DNA labeling kit (Takara). After washing in 2 × SSC/0.1% SDS and 0.1 × SSC/0.1% SDS, filters were exposed onto IP plates (Fuji Film, Tokyo, Japan) and analyzed using a BAS1800 system (Fuji Film).

**Real-time PCR.** TaqMan real-time PCR was performed as described previously.[24] Single-stranded cDNA was synthesized from total RNA using a High-Capacity cDNA Archive Kit (Applied Biosystems, Foster City, CA, USA). Quantitative real-time PCR was performed using an ABI PRISM® 7900HT Sequence Detection System (Applied Biosystems) with a TaqMan Universal PCR Master Mix (Applied Biosystems) according to the manufacturer's protocol. The expressions of mRNAs were measured by real-time PCR using the Applied Biosystems Assays-on-Demand™ Gene Expression Product. The thermal cycler conditions were as follows: 2 min at 50°C and then 10 min at 95°C, followed by two-step PCR for 50 cycles consisting of 95°C for 15 s followed by 60°C for 1 min. For each PCR, we checked the slope value, $R^2$ value, and linear range of a standard curve of serial dilutions. All reactions were performed in duplicate. The results are expressed relative to the β-actin, internal control.

**Immunoblot analysis.** Cells were washed with PBS, harvested and lysed in Nonidet P-40 lysis buffer (1% Nonidet P-40, 20 mM HEPES (pH 7.6), 100 mM NaCl, 3 mM $MgCl_2$, 5 mM dithiothreitol, and 0.1% protease inhibitor cocktail (Sigma)). Lysates were then sonicated on ice three times for 5 s and centrifuged at 15 000 r.p.m. for 5 min. Supernatants were retained and boiled for 5 min in SDS sample buffer. Equal amounts of protein were subjected to 10–15% SDS-PAGE, transferred to PVDF membranes, and immunoblotted with each primary antibody. Membranes were washed with TBS/Tween-20, and then incubated with an alkaline phosphatase-conjugated secondary antibody (Sigma). The corresponding bands were detected using ECL Plus Western Blotting Detection System (GE Healthcare UK Ltd, Buckinghamshire, England). The density of each band was quantified using the Scion Image Program (Scion Corporation). As primary antibodies, anti-PERK antibody was provided by Dr. David Ron (New York University) and anti-IRE1α antibody was provided by Dr. Fumihiko Urano (University of Massachusetts Medical School). Anti-KDEL (Stressgen, Victoria, BC, Canada), anti-total eIF2α (Cell signaling Technology, Beverly, MA, USA), anti-eIF2α (phosphospecific) (Stressgen), anti-ATF6α (Santa Cruz Biotechnology, Santa Cruz, CA, USA), anti-ATF6β (Santa Cruz Biotechnology), anti-TX (MBL Co. Ltd, Nagoya, Japan), and anti-actin (Chemicon, Temecula, CA, USA) antibodies were purchased commercially. Anti-KDEL antibody detected BiP and GRP94. Anti-TX antibody detected caspase 4 protein.

**Caspase activity.** SK-N-SH cells were seeded into 96-well culture plates ($1.0 \times 10^4$ cells/well). Cells were cultured under standard conditions for 12 h, and then treated with 5 μM BIX or vehicle for another 12 h. After BIX or vehicle treatment, the whole medium was replaced with fresh medium containing 0.5 μg/ml Tm and cells were incubated for additional 36 or 48 h. After incubation, caspase-3 and -7 activity was measured using a caspase-Glo 3/7 Assay kit (Promega), according to the manufacturer's instructions. Luminescent signals were measured using a luminometer (Berthold Technologies). The measurement of caspases 3 and 7 activities was conducted in three independent experiments.

**Cell death assay.** SK-N-SH cells were pretreated with 5 μM BIX or vehicle for 12 h, after which the whole medium was replaced with fresh medium containing 0.5 μg/ml Tm, in which cell were cultured for the indicated times. Cells were fixed with 4% paraformaldehyde for 30 min at 4°C, washed with PBS for 5 min, and then stained with 100 μM Hoechst 33258 (Wako Pure Chemical Co., Tokyo, Japan) in PBS for 20 min. A total of 500 cells were counted randomly and apoptotic cells were determined by fluorescence microscopy.

**Focal cerebral ischemia model in mice.** Male adult ddY mice weighing 24–34 g (Japan SLC) were used in experiments, and were housed under diurnal lighting conditions. Anesthesia was induced by 2.0% isoflurane, then maintained using 1% isoflurane in 70% $N_2O$ and 30% $O_2$ using an animal general anesthesia machine (Soft Lander, Sin-ei Industry Co. Ltd, Saitama, Japan). Body temperature was maintained between 37.0 and 37.5°C with the aid of a heating pad and heating lamp. A filament occlusion of the left MCA was carried out as previously

described.[25,26] Briefly, the left MCA was occluded with an 8-0 nylon monofilament (Ethicon, Somerville, NJ, USA) coated with a mixture of silicone resin (Xantopren; Bayer Dental, Osaka, Japan). This coated filament was introduced into the internal carotid artery through the common carotid artery up to the origin of the anterior cerebral artery, so as to occlude the MCA and posterior communicating artery. At the same time, the left common carotid artery was occluded by the suture. Permanent ischemia was selected because it produced a reproducible subtotal infarction in our previous studies.[25,26] Twenty-four hours after the occlusion, the forebrain was divided into five coronal 2 mm sections using a mouse brain matrix (RBM-2000C; Activational Systems, Warren, MI, USA). Sections were then stained with 2% TTC. Images of the infarcted areas were recorded using a digital camera (Nikon, COOLPIX4500), quantitated using Image J software (http://rsb.info.nih.gov/ij/download/), and calculated as in a previous report.[26] Brain swelling was calculated according to the following formula: (infarct volume + ipsilateral undamaged volume−contralateral volume) × 100/contralateral volume (%).[25] BIX was dissolved in 10% DMSO and fresh solution was made daily. DMSO (10%) was used as a control. Physiologic parameters were recorded according to our previously described method.[23] In brief, a polyethylene catheter was inserted into the femoral artery to sample arterial blood (30 $\mu$l) and measure blood pressure. After the catheter had been inserted into the femoral artery, 2 $\mu$l of BIX at 2.5 or 10 $\mu$g/$\mu$l was intracerebroventricularly administered 30 min before the start of the ischemia, because we do not know the permeability of BIX to the blood brain barrier. Body temperature, arterial blood pressure, $pO_2$, $pCO_2$, pH, and plasma glucose were measured 15 min after the start of the ischemia. There were no significant differences in physiological parameters between the vehicle- and BIX-treated groups (data not shown). After 30 min of ischemia, vehicle- and BIX-treated mice exhibited moderate neurological deficits (such as circling, decreased resistance to lateral pushing, decreased locomotor activity, flexion of the right (contralateral to the ischemia) torso and forelimb upon lifting the animal by its tail, and abnormal posture). Animals showing no neurological deficits at 30 min after the occlusion were removed from the study on the grounds that they had not undergone successful occlusion of the MCA. We removed 2 out of 15, 1 out of 13, and 1 out of 13 mice in control, 5 $\mu$g BIX-treated, and 20 $\mu$g BIX-treated groups, respectively. The present experiments were performed in accordance with the Guidelines for Animal Experiments of Gifu Pharmaceutical University.

**Neurological deficits.** Mice were tested for neurological deficits at 24 h after MCA occlusion and scored as described previously[25] using the following scale: 0 = no observable neurological deficits (normal); 1 = failure to extend the right forepaw (mild); 2 = circling to the contralateral side (moderate); 3 = loss of walking or righting reflex (severe). The investigator who rated the mice was blinded as to the group to which each mouse belonged.

**Immunohistochemistry.** At 24 h after MCA occlusion, mice were injected with sodium pentobarbital (nembutal; 50 mg/kg, i.p.), and then perfused through the left ventricle with 4% paraformaldehyde in 0.1 M phosphate buffer (PB; pH 7.4). Brains were removed after 15 min of perfusion fixation at 4°C and immersed in the same fixative solution overnight at 4°C. They were then immersed in 25% sucrose in 0.1 M PB for 24 h, and finally frozen in powdered dry ice. Coronal sections (10 $\mu$m) were cut on a cryostat at −20°C and stored at −80°C until use. After rehydration, endogenous peroxidase activity was quenched using 1% hydrogen peroxidase in methanol. Next, brain sections were blocked with 3% BSA in PBS/0.1% Triton X-100 for 1 h, and then incubated overnight at 4°C with primary antibody in the same buffer. Sections were washed and then incubated with biotinylated secondary antibody before being incubated for 30 min at room temperature with avidin–biotin–peroxidase complex, and then developed using diaminobenzidine (DAB) peroxidase substrate. Caspase 3-stained cells were counted in the striatum. The results are expressed as positive cells per 1 mm$^2$.

**TUNEL staining.** Apoptosis was detected using the TUNEL method using an *in situ* cell death detection kit, POD (Roche, Penzberg, Germany). TUNEL signals were developed using a DAB peroxidase substrate kit (Vector Labs, Burlingame, CA, USA).

***In situ* hybridization histochemistry.** CHOP and GAPDH cDNAs were subcloned into pGEM-T Easy and pBluescript vectors, respectively. Digoxigenin-labeled cRNA probes were made by *in vitro* transcription in the presence of digoxigenin using subcloned cDNAs for these genes as templates. *In situ* hybridization using digoxigenin-labeled cRNA probes was performed as previously described.[27]

**Statistical analysis.** Statistical comparisons were made using a one-way ANOVA followed by a Student's *t*-test, Dunnett's test, or the Mann–Whitney *U*-test. STATVIEW version 5.0 (SAS Institute Inc., Cary, NC, USA) was used for statistical analyses. $P<0.05$ was considered to indicate statistical significance.

**Acknowledgements.** We thank Dr. David Ron for the PERK$^{-/-}$ MEFs and the anti-PERK antibody, Dr. Fumihiko Urano for the IRE1$^{-/-}$ MEFs and the anti-IRE1$\alpha$ antibody, Dr. Laurie H Glimcher for the ATF6$\alpha\beta$/MEFs, and Dr. K Mori for the BiP-pGL3 reporter plasmid. We also thank Ms Mikiko Kubo for her technical assistance. This work was supported by a Grant-in-Aid for Scientific Research (17200026) from the Japan Society for the Promotion of Science and Research on Psychiatric and Neurological Diseases and Mental Health from the Japan Ministry of Health, Labor, and Welfare. This study was supported by the Program for Promotion of Fundamental Studies in Health Sciences of the National Institute of Biomedical Innovation. Funding was also provided by the Japan Society for the Promotion of Science (SK).

1. Zhang K, Kaufman RJ. The unfolded protein response: a stress signaling pathway critical for health and disease. *Neurology* 2006; **66** (Suppl 1): s102–s109.
2. Katayama T, Imaizumi K, Sato N, Miyoshi K, Kudo T, Hitomi J *et al*. Presenilin-1 mutations downregulate the signalling pathway of the unfolded-protein response. *Nat Cell Biol* 1999; **8**: 479–485.
3. Katayama T, Imaizumi K, Honda A, Yoneda T, Kudo T, Takeda M *et al*. Disturbed activation of endoplasmic reticulum stress transducers by familial Alzheimer's disease-linked presenilin 1 mutations. *J Biol Chem* 2001; **276**: 43446–43454.
4. Yasuda Y, Kudo T, Katayama T, Imaizumi K, Yatera M, Okochi M *et al*. FAD-linked presenilin-1 mutants impede translation regulation under ER stress. *Biochem Biophys Res Commun* 2002; **296**: 313–318.
5. Hitomi J, Katayama T, Eguchi Y, Kudo T, Taniguchi M, Koyama Y *et al*. Involvement of caspase-4 in endoplasmic reticulum stress-induced apoptosis and A$\beta$-induced cell death. *J Cell Biol* 2004; **165**: 347–356.
6. Kitada T, Asakawa S, Hattori N, Matsumine H, Yamamura Y, Minoshima S *et al*. Mutations in the Parkin gene cause autosomal recessive juvenile Parkinsonism. *Nature* 1998; **392**: 605–608.
7. Imai Y, Soda M, Inoue H, Hattori N, Mizuno Y, Takahashi R. An unfolded putative transmembrane polypeptide, which can lead to endoplasmic reticulum stress, is a substrate of Parkin. *Cell* 2001; **105**: 891–902.
8. Nishitoh H, Matsuzawa A, Tobiume K, Saegusa K, Takeda K, Hori S *et al*. ASK1 is essential for endoplasmic reticulum stress-induced neuronal cell death triggered by expanded polyglutamine repeats. *Gene Dev* 2002; **16**: 1345–1355.
9. Bence NF, Sampat RM, Kopito RR. Impairment of the ubiquitin–proteasome system by protein aggregation. *Science* 2001; **292**: 1552–1555.
10. Kumar R, Azam S, Sullivan JM, Owen C, Cavener DR, Zhang P *et al*. Brain ischemia and reperfusion activates the eukaryotic initiation factor 2alpha kinase, PERK. *J Neurochem* 2001; **77**: 1418–1421.
11. Paschen W, Aufenberg C, Hotop S, Mengesdorf T. Transient cerebral ischemia activates processing of xbp1 messenger RNA indicative of endoplasmic reticulum stress. *J Cereb Blood Flow Metab* 2003; **23**: 449–461.
12. Boyce M, Bryant KF, Jousse C, Long K, Harding HP, Scheuner D *et al*. A selective inhibitor of eIF2$\alpha$ dephosphorylation protects cells from ER stress. *Science* 2005; **307**: 935–939.
13. Kim AJ, Shi Y, Austin RC, Werstuck GH. Valproate protects cells from ER stress-induced lipid accumulation and apoptosis by inhibiting glycogen synthase kinase-3. *J Cell Sci* 2005; **118**: 89–99.
14. ZaiFang Y, Luo H, Weiming F, Mattson MP. The endoplasmic reticulum stress-responsive protein GRP78 protects neurons against excitotoxicity and apotosis: suppression of oxidative stress and stabilization of calcium homeostasis. *Exp Neurol* 1999; **155**: 302–314.
15. Rao RV, Peel A, Logvinova A, del Rio G, Hermel E, Yokota T *et al*. Coupling endoplasmic reticulum stress to the cell death program: role of the ER chaperone GRP78. *FEBS Lett* 2002; **514**: 122–128.
16. Reddy RK, Mao C, Baumeister P, Austin RC, Kaufman RJ, Lee AS. Endoplasmic reticulum chaperone protein GRP78 protects cells from apoptosis induced by topoisomerase inhibitors: role of ATP binding site in suppression of caspase-7 activation. *J Biol Chem* 2003; **278**: 20915–20924.
17. Gomer C, Ferrario A, Rucker N, Wong S, Lee AS. Glucose regulated protein induction and cellular resistance to oxidative stress mediated by porphyrin photosensitization. *Cancer Res* 1991; **51**: 6574–6579.
18. Li LJ, Li X, Ferrario A, Rucker N, Liu ES, Wong S *et al*. Establishment of a Chinese hamster ovary cell line that expresses grp78 antisense transcripts and suppresses A23187 induction of both GRP78 and GRP94. *J Cell Physiol* 1992; **153**: 575–582.

19. Sugawara S, Takeda K, Lee A, Dennert G. Suppression of stress protein GRP78 induction in tumor B/C10ME eliminates resistance to cell mediated cytotoxicity. *Cancer Res* 1993; **53**: 6001–6005.
20. DeGracia DJ, Montie HL. Cerebral ischemia and the unfolded protein response. *J Neurochem* 2004; **91**: 1–8.
21. Kaufman RJ. Orchestrating the unfolded protein response in health and disease. *J Clin Invest* 2002; **110**: 1389–1398.
22. Tajiri S, Oyadomari S, Yano S, Morioka M, Gotoh T, Hamada JI *et al.* Ischemia-induced neuronal cell death is mediated by the endoplasmic reticulum stress pathway involving CHOP. *Cell Death Differ* 2004; **11**: 403–415.
23. Bertolotti A, Zhang Y, Hendershot LM, Harding HP, Ron D. Dynamic interaction of BiP and ER stress transducers in the unfolded-protein. *Nat Cell Biol* 2000; **2**: 326–332.
24. Chen D, Padiernos E, Ding F, Lossos IS, Lopez CD. Apoptosis-stimulating protein of p53-2 ($ASPP2^{ASPP2}$) is an E2F target gene. *Cell Death Differ* 2005; **12**: 358–368.
25. Hara H, Huang PL, Panahian N, Fishman MC, Moskowitz MA. Reduced brain edema and infarction volume in mice lacking the neuronal isoform of nitric oxide synthase after transient MCA occlusion. *J Cereb Blood Flow Metab* 1996; **16**: 605–611.
26. Hara H, Friedlander RM, Gagliardini V, Ayata C, Fink K, Huang Z *et al.* Inhibition of interleukin 1$\beta$ converting enzyme family proteases reduces ischemic and excitotoxic neuronal damage. *Proc Natl Acad Sci USA* 1997; **94**: 2007–2012.
27. Honma Y, Kanazawa K, Mori T, Tanno Y, Tojo M, Kiyosawa H *et al.* Identification of a novel gene, OASIS, which encodes for a putative CREB/ATF family transcription factor in the long-term cultured astrocytes and gliotic tissue. *Brain Res Mol Brain Res* 1999; **69**: 93–103.

# Effect of an Inducer of BiP, a Molecular Chaperone, on Endoplasmic Reticulum (ER) Stress-Induced Retinal Cell Death

*Yuta Inokuchi,[1] Yoshimi Nakajima,[1] Masamitsu Shimazawa,[1] Takanori Kurita,[2] Mikiko Kubo,[3] Atsushi Saito,[4] Hironao Sajiki,[2] Takashi Kudo,[5] Makoto Aihara,[5] Kazunori Imaizumi,[4] Makoto Araie,[5] and Hideaki Hara[1]*

**Purpose.** The effect of a preferential inducer of 78 kDa glucose-regulated protein (GRP78)/immunoglobulin heavy-chain binding protein (BiP; BiP inducer X, BIX) against tunicamycin-induced cell death in RGC-5 (a rat ganglion cell line), and also against tunicamycin- or *N*-methyl-D-aspartate (NMDA)-induced retinal damage in mice was evaluated.

**Methods.** In vitro, BiP mRNA was measured after BIX treatment using semi-quantitative RT-PCR or real-time PCR. The effect of BIX on tunicamycin (at 2 μg/mL)-induced damage was evaluated by measuring the cell-death rate and CHOP protein expression. In vivo, BiP protein induction was examined by immunostaining. The retinal cell damage induced by tunicamycin (1 μg) or NMDA (40 nmol) was assessed by examining ganglion cell layer (GCL) cell loss, terminal deoxyribonucleotidyl transferase (TdT)-mediated dUTP nick-end labeling (TUNEL) staining, and CHOP protein expression.

**Results.** In vitro, BIX preferentially induced BiP mRNA expression both time- and concentration-dependently in RGC-5 cells. BIX (1 and 5 μM) significantly reduced tunicamycin-induced cell death, and BIX (5 μM) significantly reduced tunicamycin-induced CHOP protein expression. In vivo, intravitreal injection of BIX (5 nmol) significantly induced BiP protein expression in the mouse retina. Co-administration of BIX (5 nmol) significantly reduced both the retinal cell death and the CHOP protein expression in GCL induced by intravitreal injection of tunicamycin or NMDA.

**Conclusions.** These findings suggest that this BiP inducer may have the potential to be a therapeutic agent for endoplasmic reticulum (ER) stress-induced retinal diseases. (*Invest Ophthalmol Vis Sci.* 2009;50:334–344) DOI:10.1167/iovs.08-2123

The endoplasmic reticulum (ER) is the cellular organelle in which proteins (destined for secretion or for diverse subcellular localizations) are not only synthesized, but acquire their correct conformation. Perturbations of the environment normally required for protein folding in the ER, or the production of large amounts of misfolded proteins exceeding the functional capacity of the organelle, trigger a pattern of physiological response in the cell, collectively known as the unfolded protein response (UPR).[1–3] The UPR serves to cope with ER stress by transcriptionally regulating ER chaperones and other ER-resident proteins, attenuating the overall translation rate, and increasing the degradation of misfolded ER proteins. ER stress is caused by the accumulation of unfolded proteins in the ER lumen, and it is associated with various neurodegenerative diseases such as Alzheimer's, Huntington's, and Parkinson's diseases, and with type-1 diabetes.[4–6] Recent reports have shown that ER stress is also involved in a variety of experimental retinal neurodegenerative models, such as those of diabetic retinopathy,[7] retinitis pigmentosa,[8,9] and glaucoma.[10,11]

Recently, we reported that BiP expression is upregulated in the retina after intravitreal injection of either tunicamycin or NMDA (a glutamate-receptor agonist).[12,13] Tunicamycin, a glucosamine-containing nucleoside antibiotic, produced by genus *Streptomyces*, is an inhibitor of *N*-linked glycosylation and the formation of *N*-glycosidic protein-carbohydrate linkages.[14] Tunicamycin, which reduces the *N*-glycosylation of proteins, causes an accumulation of unfolded proteins in the ER and thus induces ER stress. Awai et al.[15] previously had demonstrated that NMDA induces CHOP protein (a member of the CCAAT/enhancer-binding protein family induced by ER stress) in GCL and the inner plexiform layer (IPL), and that CHOP$^{-/-}$ mice are more resistant to NMDA-induced retinal cell death than wild-type mice. These findings indicate that ER stress may be involved in these models of retinal injury.

BiP, a highly conserved member of the 70 kDa heat shock protein family, is one of the chaperones localized to the ER membrane,[16,17] and it is a major ER-luminal $Ca^{2+}$-storage protein.[18,19] BiP works to restore folding in misfolded or incompletely assembled proteins,[20–22] the interaction between BiP and misfolded proteins being dependent on its hydrophobic motifs.[23–25] Proteins stably bound to BiP are subsequently translocated from the ER into the cytosol, where they are degraded by proteasomes.[26,27] Previous reports have show that induction of BiP prevents the neuronal death induced by ER stress.[28–31] Hence, a selective inducer of BiP might attenuate ER stress and be a new, useful therapeutic agent for the treatment of ER stress-associated diseases.

This seemed an interesting idea, and we recently identified BiP inducer X (BIX) while screening for low molecular

From the Departments of [1]Biofunctional Evaluation, Molecular Pharmacology and [2]Medicinal Chemistry, Gifu Pharmaceutical University, Gifu, Japan; [3]Department of Psychiatry, Osaka University Graduate School of Medicine, Osaka, Japan; [4]Division of Molecular and Cellular Biology, Department of Anatomy, Faculty of Medicine, University of Miyazaki, Miyazaki, Japan; and [5]Department of Ophthalmology, University of Tokyo School of Medicine, Tokyo, Japan.

Supported in part by a Grant-in-Aid (No.18209053) for scientific research from the Ministry of Education, Science, Sports, Culture of the Japanese Government; by a research grant (No.18210101) from the Ministry of Health, Labor, and Welfare of the Japanese Government, and by Grant-in-Aid for Japan Society for the Promotion of Science Fellows.

Submitted for publication April 4, 2008; revised July 25, 2008; accepted October 27, 2008.

Disclosure: **Y. Inokuchi**, None; **Y. Nakajima**, None; **M. Shimazawa**, None; **T. Kurita**, None; **M. Kubo**, None; **A. Saito**, None; **H. Sajiki**, None; **T. Kudo**, None; **M. Aihara**, None; **K. Imaizumi**, None; **M. Araie**, None; **H. Hara**, None

The publication costs of this article were defrayed in part by page charge payment. This article must therefore be marked "*advertisement*" in accordance with 18 U.S.C. §1734 solely to indicate this fact.

Corresponding author: Hideaki Hara, Department of Biofunctional Evaluation, Molecular Pharmacology, Gifu Pharmaceutical University, 5-6-1 Mitahora-higashi, Gifu 502-8585, Japan; hidehara@gifu-pu.ac.jp.



Investigative Ophthalmology & Visual Science, January 2009, Vol. 50, No. 1

mass compounds that might induce BiP using high-throughput screening (HTS) with a BiP reporter assay system (Dual-Luciferase Reporter Assay; Promega Corporation, Madison, WI).[32] We found that BIX preferentially induced BiP mRNA and protein in SK-N-SH cells and reduced tunicamycin-induced cell death. Intracerebroventricular pretreatment with BIX reduced the infarction size after focal cerebral ischemia in mice. In view of the retinal research described above, we wondered whether BIX might reduce the retinal ganglion cell loss and CHOP expression induced by tunicamycin or NMDA treatment.

In the present study, we examined primarily whether induction of BiP might inhibit the retinal cell death induced by tunicamycin in RGC-5 cells in vitro, and/or that induced by tunicamycin or NMDA in mice in vivo.

## Materials and Methods

All experiments were performed in accordance with the ARVO Statement for the Use of Animals in Ophthalmic and Vision Research, and they were approved and monitored by the Institutional Animal Care and Use Committee of Gifu Pharmaceutical University, Gifu, Japan.

### Materials

Dulbecco modified Eagle medium (DMEM) and NMDA were purchased from Sigma-Aldrich (St. Louis, MO). The other drugs used and their sources were as follows: BIX, 1-(3,4-dihydroxyphenyl)-2-thiocyanatoethanone, was synthesized in the Department of Medicinal Chemistry, Gifu Pharmaceutical University, while tunicamycin was purchased from Wako (Osaka, Japan). Isoflurane was acquired from Nissan Kagaku (Tokyo, Japan) and fetal bovine serum (FBS) was from Valeant (Costa Mesa, CA).

### RGC-5 Culture

RGC-5[32] were gifted by Neeraj Agarwal (Department of Pathology and Anatomy, UNT Health Science Center, Fort Worth, TX). Cultures of RGC-5 were maintained in DMEM supplemented with 10% FBS, 100 U/mL penicillin (Meiji Seika Kaisha Ltd., Tokyo, Japan), and 100 μg/mL streptomycin (Meiji Seika Kaisha, Ltd.) in a humidified atmosphere of 95% air and 5% $CO_2$ at 37°C. The RGC-5 cells were passaged by trypsinization every 3 days, as in our previous reports.[12,15,33] We used RGC-5 without any differentiation.

### RNA Isolation and Semi-Quantitative RT-PCR Analysis

To examine the effect of BIX on BiP mRNA expression, RGC-5 cells were seeded in six-well plates at a density of $1.4 \times 10^5$ cells per well. After the cells had been incubating for 24 h, they were exposed to 50 μM BIX in 1% FBS DMEM for 0.5, 1, 2, 4, 6, 8, or 12 h, or to 2, 10, 50, or 150 μM BIX in 1% FBS DMEM for 6 h. Total RNA was extracted (RNeasy Mini Kit; QIAGEN KK, Tokyo, Japan) according to the manufacture's protocol. The total RNA was divided into microtubes, and frozen to −80°C. RNA concentrations were determined spectrophotometrically at 260 nm. First-strand cDNA was synthesized in a 20-μl reaction volume using a random primer (Takara, Shiga, Japan) and Moloney murine leukemia virus reverse transcriptase (Invitrogen, Carlsbad, CA). PCR was performed in a total volume of 30 μL containing 0.8 μM of each primer, 0.2 mM dNTPs, 3 U *Taq* DNA polymerase (Promega), 2.5 mM $MgCl_2$, and 1× PCR buffer. The amplification conditions for the semi-quantitative RT-PCR analysis were as follows: an initial denaturation step (95°C for 5 minutes), 20 cycles of 95°C for 1 minute, 55°C for 1 minute, and 72°C for 1 minute, and a final extension step (72°C for 7 minutes). The numbers of amplification cycles for the detection of BiP and β-actin were 18 and 15, respectively. The primers used for amplification were as follows: BiP: 5'-GTTTGCTGAGGAAGACAAAAAGCTC-3' and 5'-CACTTCCATAGAGTTTGCTGATAATTG-3'; β-actin: 5'-TCCTCCCTGGAGAAGAGCTAC-3' and 5'-TCCTGCTTGCTGATCCACAT-3'.

PCR products were resolved by electrophoresis through 6% (w/v) polyacrylamide gels. The density of each band was quantified using an imaging program (Scion Image Program; Scion Corporation, Frederick, MD).

### Real-Time PCR

Real-time PCR (TaqMan; Applied Biosystems, Foster City, CA) was performed as described previously.[34] Single-stranded cDNA was synthesized from total RNA using a high-capacity cDNA archive kit (Applied Biosystems). Quantitative real-time PCR was performed using a sequence detection system (ABI PRISM 7900HT; Applied Biosystems) with a PCR master mix (TaqMan Universal PCR Master Mix; Applied Biosystems), according to the manufacturer's protocol. mRNA expression was measured by real-time PCR using a gene expression product (Assays-on-Demand Gene Expression Product; Applied Biosystems) and a BiP probe (Assay ID Details: Mm00517691). The thermal cycler conditions were as follows: 2 minutes at 50°C and then 10 minutes at 95°C, followed by two-step PCR for 50 cycles consisting of 95°C for 15 seconds followed by 60°C for 1 minute. For each PCR, we obtained the slope value, $R^2$ value, and linear range of a standard curve of serial dilutions. All reactions were performed in duplicate. The results are expressed relative to the β-actin (Assay ID Details: Mm00661904) internal control.

### Cell Viability

To examine the effects of BIX on the cell death induced by tunicamycin (2 μg/mL) or staurosporine (an ER stress-independent apoptosis inducer, 30 nm) RGC-5 cells were seeded at a low density of 700 cells per well into 96-well plates. After pretreatment with BIX for 12 h, tunicamycin or staurosporine was added to the cultures for 48 h or 24 h, respectively. Cell death was assessed on the basis of combination staining with the fluorescent dyes Hoechst 33342 and propidium iodide (PI; Molecular Probes, Eugene, OR) or the change in fluorescence intensity after the cellular reduction of WST-8 to formazan. Hoechst 33342 (λex 350 nm, λem 461 nm) and PI (λex 535 nm, λem 617 nm) were added to the culture medium at final concentrations of 8 and 1.5 μM, respectively, for 30 minutes. Images were collected using a CCD camera (DP30VW; Olympus America, Center Valley, PA) via an epifluorescence microscope (IX70; Olympus, Tokyo, Japan) fitted with fluorescence filters for Hoechst 33342 (U-MWU; Olympus), and PI (U-MWIG; Olympus). In WST-8 assay, cell viability was assessed by culturing cells in a culture medium containing 10% WST-8 (Cell Counting Kit-8; Dojin Kagaku, Kumamoto, Japan) for 3 h at 37°C, with quantification being achieved by scanning with a microplate reader at 492 nm.[35] This absorbance is expressed as a percentage of that in control cells (which were in 1% FBS DMEM) after subtraction of background absorbance.

### Animals

Mice used were male adult ddY mice (Japan SLC, Hamamatsu, Japan), male adult Thy-1-cyan fluorescent protein (CFP) transgenic mice (The Jackson Laboratory, Bar Harbor, Maine),[36] and ER stress-activated indicator (ERAI)-transgenic mice carrying the F-XBP1ΔDBD-venus, a variant of green fluorescent protein (GFP) fusion gene, which allows effective identification of cells under ER stress in vivo, as previously described by Iwawaki et al.[37] Briefly, when ER stress in ERAI transgenic mice was induced, splicing of mRNA encoding the XBP-1 fusion gene occurs and the spliced form of F-XBP1ΔDBD-venus fusion gene could be translated into fluorescent protein. Thus, it is visualized by the fluorescence intensity arising from the XBP-Δ-venus fusion protein during ER stress, and we measured it by fluorescence microscopy and immunoblotting in the present study.

All mice were kept under controlled lighting conditions (12 h:12 h light/dark). The mouse genotype was determined by applying standard PCR methodology to tail DNA.

## NMDA- or Tunicamycin-Induced Retinal Damage

NMDA- or tunicamycin-induced retinal damage was produced as previously reported by Siliprandi et al. (1992).[38] Briefly, mice were anesthetized with 3.0% isoflurane and maintained with 1.5% isoflurane in 70% $N_2O$ and 30% $O_2$ via an animal general anesthesia machine (Soft Lander; Sin-ei Industry Co. Ltd., Saitama, Japan). The body temperature was maintained between 37.0 and 37.5°C with the aid of a heating pad. Retinal damage was induced by the injection (2 μL/eye) of NMDA (Sigma-Aldrich) at 20 mM or tunicamycin at 1 μg/mL dissolved in 0.01 M PBS with 5% dimethyl sulfoxide (DMSO). Each solution was injected into the vitreous body of the left eye under the above anesthesia. One drop of 0.01% levofloxacin ophthalmic solution (Santen Pharmaceuticals Co. Ltd., Osaka, Japan) was applied topically to the treated eye immediately after the intravitreal injection. Seven days after the injection, eyeballs were enucleated for histologic analysis. For comparative purposes, nontreated retinas from each mouse strain were also investigated. BIX (0.5 or 5 nmol) or vehicle (5% DMSO in PBS) was co-administered with the NMDA or tunicamycin in each mouse.

## Histologic Analysis

In mice under anesthesia produced by an intraperitoneal injection of sodium pentobarbital (80 mg/kg), each eye was enucleated and kept immersed for at least 24 h at 4°C in a fixative solution containing 4% paraformaldehyde. Six paraffin-embedded sections (thickness, 4 μm) cut through the optic disc of each eye were prepared in a standard manner and stained with hematoxylin and eosin. The damage induced by NMDA or tunicamycin was then evaluated, with three sections from each eye being used for the morphometric analysis, as described below. Light-microscope images were photographed, and the cells in the GCL at a distance between 375 and 625 μm from the optic disc were counted on the photographs in a masked fashion by a single observer (Y.I.). Data from three sections (selected randomly from the six sections) were averaged for each eye and used to evaluate the cell count in the GCL.

## Retinal Flatmounts and Analysis in Transgenic Mice

Transgenic mice were given an overdose of sodium pentobarbital, and retinas were dissected out and fixed for 30 minutes in 4% paraformaldehyde diluted in 0.1 M phosphate buffer (PB) at pH 7.4. Retinas were subsequently washed with PBS at room temperature, flatmounted on clean glass slides using fluorescent mounting medium (Dako Corp., Carpinteria, CA), and stored in the dark at 4°C for 1 week. The damage induced by tunicamycin was then evaluated, with four sections (dorsal, ventral, temporal, and nasal) from each eye being used for the morphometric analysis, as described below. At various times after intravitreal injections (24 h in ERAI mice and 7 days in Thy-1-CFP transgenic mice), fluorescent images were photographed (×200, 0.144 $mm^2$) using an epifluorescence microscope (BX50; Olympus) fitted with a CCD camera (DP30VW; Olympus). In the case of Thy-1-CFP transgenic mice, Thy-1-CFP-positive cells at a distance of 1 mm from the optic disc were counted on the photographs in a masked fashion by a single observer (Y.I.). Data from the four parts of each eye were used to evaluate the RGC count.[39]

## Immunostaining

Eyes were enucleated as described under Histologic Analysis, fixed in 4% paraformaldehyde overnight at 4°C, immersed in 25% sucrose for 48 h at 4°C, and embedded in optimum cutting temperature (OCT) compound (Sakura Finetechnical Co. Ltd, Tokyo, Japan). Transverse 10-μm thick cryostat sections were cut and placed onto slides (MAS COAT; Matsunami Glass Ind., Ltd., Osaka, Japan). Immunohistochemical staining was performed according to the following protocol: Briefly, tissue sections were washed in 0.01 M PBS for 10 minutes, and then endogenous peroxidase was quenched by treating the sections with 3% hydrogen peroxide in absolute methanol for 10 minutes, followed by a pre-incubation with 10% normal goat serum. They were then incubated overnight at 4°C with the following primary antibodies: against CHOP (1:1000 dilution in PBS; Santa Cruz, CA), and against BiP/GRP78 (1:1000 dilution in PBS; BD Transduction Laboratories, Lexington, KY). Sections were washed and then incubated with biotinylated anti-rabbit IgG or anti-mouse IgG. They were subsequently incubated with the avidin-biotin-peroxidase complex for 30 minutes, and then developed using diaminobenzidine (DAB) peroxidase substrate. Images were obtained using a digital camera (COOLPIX 4500; Nikon, Tokyo, Japan).

## Quantitation of Density

In the DAB-labeled areas of anti-BiP/GRP78 (BD Transduction Laboratories) and anti-CHOP (Santa Cruz) in the GCL and IPL at a distance between 475 and 525 μm (50 × 50 μm) from the optic disc, retinal DAB-labeled cell density was evaluated by means of appropriately calibrated computerized image analysis, using median density in the range of 0 to 255 as an analysis tool (Image Processing and Analysis in Java, Image J; National Institute of Mental Health, Bethesda, MD) and averaged for two areas.[40] The data lie within the dynamic range of this assays.

Briefly, light-microscope images of the above-mentioned areas were photographed, inverted in a gradation sequence using image editing software (Adobe Photoshop 5.5; Adobe Systems Inc., San Jose, CA), and then optical intensity was evaluated using Image J. The score for the negative-control (nontreated with first antibody), as the background value, was subtracted from the scores.

## TUNEL Staining

TUNEL staining was performed according to the manufacturer's protocol (In Situ Cell Death Detection Kit; Roche Biochemicals, Mannheim, Germany) to detect the retinal cell death induced by NMDA. Mice were anesthetized with pentobarbital sodium at 80 mg/kg, IP, 24 h after intravitreal injection (either of NMDA 40 nmol/eye or of tunicamycin 1 μg/eye). The eyes were enucleated, fixed overnight in 4% paraformaldehyde, and immersed for 2 days in 25% sucrose with PBS. The eyes were then embedded in a supporting medium (OCT compound) for frozen-tissue specimens. Retinal sections at 10-μm thick were cut on a cryostat at −25°C, and stored at −80°C until staining. After twice washing with PBS, sections were incubated with terminal TdT enzyme at 37°C for 1 h, then washed 3 times in PBS for 1 minute at room temperature. Sections were subsequently incubated with an anti-fluorescein antibody-peroxidase conjugate at room temperature in a humidified chamber for 30 minutes, then developed using DAB tetrahydrochloride peroxidase substrate. Light-microscope images were photographed, and the labeled cells in the GCL at a distance between 375 and 625 μm from the optic disc were counted in two areas of the retina in a masked fashion by a single observer (Y.I.). The number of TUNEL-positive cells was averaged for these two areas, and plotted as the number of TUNEL-positive cells.

## Western Blot Analysis

RGC-5 cells were lysed using a cell-lysis buffer (RIPA buffer R0278; Sigma-Aldrich) with protease (P8340; Sigma-Aldrich) and phosphatase inhibitor cocktails (P2850 and P5726; Sigma-Aldrich), and 1 mM EDTA. In vivo, mice were euthanized using sodium pentobarbital at 80 mg/kg, IP, and their eyeballs were quickly removed. The retinas were carefully separated from the eyeballs and quickly frozen in dry ice. For protein extraction, the tissue was homogenized in the cell-lysis buffer using a homogenizer (Physcotron; Microtec Co. Ltd., Chiba, Japan). The lysate was centrifuged at 12,000*g* for 20 minutes, and the supernatant was used for this study. Assays to determine the protein concentration were performed by comparison with a known concentration of bovine serum albumin using a BCA protein assay kit (Pierce Biotechnology, Rockford, IL). A mixture of equal parts of an aliquot of

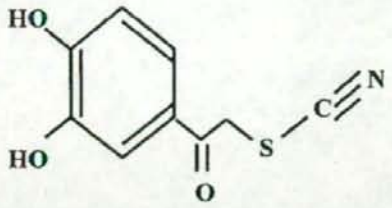


FIGURE 1. The structure of BIX (1-(3,4-dihydroxyphenyl)-2-thiocyanate-ethanone).

protein and sample buffer with 10% 2-mercaptoethanol was subjected to 10% sodium dodecyl sulfate-polyacrylamide gel electrophoresis. The separated protein was then transferred onto a polyvinylidene difluoride membrane (Immobilon-P; Millipore Corporation, Bedford, MA). For immunoblotting, the following primary antibodies were used: rabbit anti-CHOP polyclonal antibody (1:1000; Santa Cruz), mouse anti-β-actin monoclonal antibody (1:4000; Sigma-Aldrich), and rabbit anti-green fluorescent protein (GFP) polyclonal antibody (1:1000; Medical & Biological Laboratories Co. Ltd., Nagoya, Japan). The secondary antibody used was either goat anti-rabbit HRP-conjugated (1:2000) or goat anti-mouse HRP-conjugated (1:2000). The immunoreactive bands were visualized using a chemiluminescent substrate (SuperSignal West Femto Maximum Sensitivity Substrate; Pierce Biotechnology). The band intensity was measured using an imaging analyzer (Lumino Imaging Analyzer; Toyobo, Osaka, Japan) and a gel analysis electrophoresis analysis software (Gel Pro Analyzer; Media Cybernetics, Atlanta, GA).

### Statistical Analysis

Data are presented as the means ± SE. Statistical comparisons were made by way of Dunnett's test or Student's *t*-test using statistical analysis software (STAT VIEW version 5.0; SAS Institute, Cary, NC). $P < 0.05$ was considered to indicate statistical significance.

## RESULTS

### BiP mRNA in RGC-5 Preferentially Induced by BIX

To clarify whether BIX (Fig. 1) induces BiP in RGC-5, we used semi-quantitative RT-PCR and real-time PCR, using a specific primer and a TaqMan probe recognizing BiP mRNA, respectively. Real-time PCR revealed that the level of BiP mRNA was significantly elevated at 0.5 to 12 h (peak at approximately 6 h) after treatment with 50 μM BIX (Fig. 2A). At 6 h after treatment with BIX (2 to 150 μM), BiP mRNA was increased concentration-dependently (Fig. 2B). Next, we used real-time *PCR* to investigate whether BIX might affect the expressions of any other genes related to the ER stress response, such as GRP94, calreticulin, protein kinase inhibitor of 58 kDa ($p58^{IPK}$), or asparagine synthetase (ASNS; Fig. 2C). Real-time PCR revealed significant inductions of ASNS and calreticulin mRNAs at 6 h after treatment with BIX at 2 and 10 μM, respectively. At 50 μM, BIX induced the mRNAs for GRP94 at 12 h, calreticulin at 6 and 12 h, $p58^{IPK}$ at 6 h, and ASNS at 12 h. In contrast, GRP94 mRNA was significantly reduced at 4 h after treatment with 50 μM BIX.

### Protective Effect of BIX against ER Stress–Induced Cell Death in RGC-5 Cells

To investigate whether BIX can prevent the cell death induced by ER stress, RGC-5 cells were pretreated for 12 h with or without BIX, then treated with 2 μg/mL tunicamycin, and finally incubated for a further 48 h. Fluorescence micrographs of Hoechst 33342 and PI staining revealed 38.4 ± 4.5% cell death ($n = 8$) at 48 h after tunicamycin treatment, (control: 0.9 ± 0.2%, $n = 8$), and pretreatment with BIX at 1 and 5 μM significantly reduced this cell death (Figs. 3A, 3B). Next, we evaluated the expression of CHOP protein after tunicamycin treatment. There was no CHOP protein expression in either nontreated or BIX-treated cells (Figs. 3C, 3D). On the other

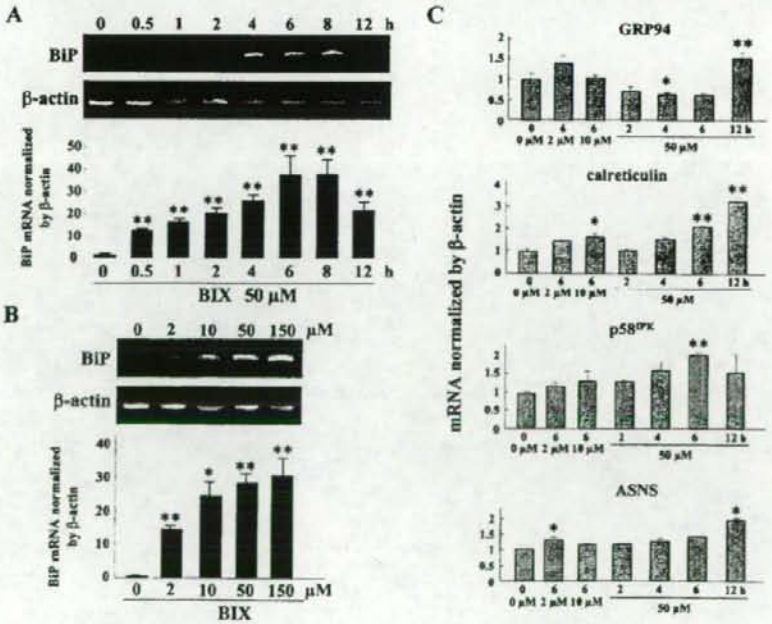


FIGURE 2. Effect of BIX on BiP mRNA expression BIX in RGC-5 cells. (A) Time-dependent induction of BiP mRNA after treatment with 50 μM BIX and (B) concentration-dependence of BIX-induced BiP mRNA expression are each shown by semi-quantitative RT-PCR (*upper panel*) and real-time PCR (*lower panel*). β-Actin mRNA is shown as an internal control. (C) Induction of GRP94, calreticulin, $p58^{IPK}$, and ASNS mRNAs at 6 h after treatment with 2 or 10 μM BIX and at 2 to 12 h after treatment with 50 μM BIX. Data are shown as mean ± SE ($n = 3$ or 4). $^*P < 0.05$, $^{**}P < 0.01$ versus 0 μM (A and B) or 0 μM/0 h (C).